J|A|C|S
ARTICLES
Published on Web 07/23/2005

Synthesis, Structure, and Reactivity of O-Donor Ir(III) Complexes: C−H Activation Studies with Benzene

Gaurav Bhalla,† Xiang Yang Liu,† Jonas Oxgaard,‡ William A. Goddard, III,‡ and Roy A. Periana*,†

Contribution from the Donald P. and Katherine B. Loker Hydrocarbon Research Institute and Department of Chemistry, University of Southern California, Los Angeles, California 90089-1661, and Materials and Process Simulation Center, Beckman Institute (139-74), Division of Chemistry and Chemical Engineering, California Institute of Technology, Pasadena, California 91125

Received March 9, 2005; E-mail: rperiana@usc.edu

Abstract: Various new thermally air- and water-stable alkyl and aryl analogues of (acac-O,O)$_2$Ir(R)(L), **R**−**Ir**−**L** (acac-O,O = κ^2-O,O-acetylacetonate, −**Ir**− is the *trans*-(acac-O,O)$_2$Ir(III) motif, **R** = CH_3, C_2H_5, Ph, $PhCH_2CH_2$, **L** = Py) have been synthesized using the dinuclear complex [Ir(μ-acac-O,O,C^3)−(acac-O,O)(acac-C^3)]$_2$, **[acac-C−Ir]$_2$**, or **acac-C−Ir−H$_2$O**. The dinuclear Ir (III) complexes, [Ir(μ-acac-O,O,C^3)−(acac-O,O)(R)]$_2$ (R = alkyl), show fluxional behavior with a five-coordinate, 16 electron complex by a dissociative pathway. The pyridine adducts, **R**−**Ir**−**Py**, undergo degenerate Py exchange via a dissociative mechanism with activation parameters for **Ph**−**Ir**−**Py** ($\Delta H^{\ddagger} = 22.8 \pm 0.5$ kcal/mol; $\Delta S^{\ddagger} = 8.4 \pm 1.6$ eu; $\Delta G^{\ddagger}_{298K} = 20.3 \pm 1.0$ kcal/mol) and **CH$_3$**−**Ir**−**Py** ($\Delta H^{\ddagger} = 19.9 \pm 1.4$ kcal/mol; $\Delta S^{\ddagger} = 4.4 \pm 5.5$ eu; $\Delta G^{\ddagger}_{298K} = 18.6 \pm 0.5$ kcal/mol). The trans complex, **Ph**−**Ir**−**Py**, undergoes quantitatively trans-cis isomerization to generate ***cis*-Ph**−**Ir**−**Py** on heating. All the **R**−**Ir**−**Py** complexes undergo quantitative, intermolecular CH activation reactions with benzene to generate **Ph**−**Ir**−**Py** and **RH**. The activation parameters ($\Delta S^{\ddagger}$ =11.5 ± 3.0 eu; $\Delta H^{\ddagger} = 41.1 \pm 1.1$ kcal/mol; $\Delta G^{\ddagger}_{298k} = 37.7 \pm 1.0$ kcal/mol) for CH activation were obtained using **CH$_3$**−**Ir**−**Py** as starting material at a constant ratio of [Py]/[C_6D_6] = 0.045. Overall the CH activation reaction with **R**−**Ir**−**Py** has been shown to proceed via four key steps: (A) pre-equilibrium loss of pyridine that generates a *trans*-five-coordinate, square pyramidal intermediate; (B) unimolecular, isomerization of the *trans*-five-coordinate to generate a *cis*-five-coordinate intermediate, ***cis*-R**−**Ir-□**; (C) rate-determining coordination of this species to benzene to generate a discrete benzene complex, ***cis*-R**−**Ir**−**PhH**; and (D) rapid C−H cleavage. Kinetic isotope effects on the CH activation with mixtures of C_6H_6/C_6D_6 (KIE = 1) and with 1,3,5-$C_6H_3D_3$ (KIE ∼3.2 at 110 °C) are consistent with this reaction mechanism.

1. Introduction

The oxidative conversion of fossilized hydrocarbons to energy and useful materials are foundational technologies. Currently, these conversions operate at high temperatures that ultimately lead to excessive emissions and high costs. Catalysts based on C−H activation[1] show potential for the development of new hydrocarbon conversion chemistry that can be substantially more efficient given the lower temperature and enhanced selectivity. While many alkane and arene CH activation systems are known, relatively few have been reported to allow efficient catalysis to generate functionalized products.[2] Some of the most efficient catalysts reported for the low-temperature, selective conversion of hydrocarbons directly to useful products, for example, alcohols, alkyl arenes and carboxylic acids, generally operate by coupling of the CH activation and functionalization steps as shown in Figure 1. Some key challenges to designing effective catalysts that operate via this sequence of reactions are (a) avoiding inhibition of the CH activation reac-

† University of Southern California.
‡ California Institute of Technology.

(1) (a) Shilov, A. E.; Shul'pin, G. B. *Activation and Catalytic Reactions of Saturated Hydrocarbons in the Presence of Metal Complexes*; Kluwer Academic: Dordrecht, 2000. (b) Shilov, A. E.; Shul'pin, G. B. *Chem. Rev.* **1997**, *97*, 2879. (c) Labinger, J. A.; Bercaw, J. E. *Nature* **2002**, *417*, 507. (d) Fulton, J. R.; Holland, A. W.; Fox, D. J.; Bergman, R. G. *Acc. Chem. Res.* **2002**, *35*, 44. (e) Crabtree, R. H. *Chem. Rev.* **1995**, *95*, 987. (f) Davies, J. A.; Watson, P. L.; Liebman, F.; Greenberg, A. *Selective Hydrocarbon Activation*; VCH: Toledo, 1990. (g) Jones, W. D. *Top. Organomet. Chem.* **1999**, *3*, 9. (h) Periana, R. A.; Bhalla, G.; Tenn, W. J., III; Young, K. J. H.; Liu, X. Y.; Mironov, O.; Jones, C.; Ziatdinov, V. R. *J. Mol. Catal. A: Chem.* **2004**, *220*, 7.

(2) For some examples, see: (a) Jia, C.; Kitamura, T.; Fujiwara, Y. *Acc. Chem. Res.* **2001**, *34*, 633. (b) Ritleng, V.; Sirlin, C.; Pfeffer, M. *Chem. Rev.* **2002**, *102*, 1731. (c) Wolf, D. *Angew Chem., Int. Ed.* **1998**, *37*, 3351. (d) Kakiuchi, F.; Murai, S. *Top. Organomet. Chem.* **1999**, *3*, 47. (e) Periana, R. A.; Mironov, O.; Taube, D.; Bhalla, G.; Jones, C. *Science*, **2003**, *30*, 814. (f) Periana, R. A.; Taube, D. J.; Gamble, S.; Taube, H.; Satoh, T.; Fujii, H. *Science* **1998**, *280*, 560−564. (g) Periana, R. A.; Taube, D. J.; Evitt, E. R.; Loffler, D. G.; Wentrcek, P. R.; Voss, G.; Masuda, T. *Science* **1993**, *259*, 340−343. (h) Chen, H. Y.; Schlecht, S.; Semple, T. C.; Hartwig, J. F. *Science* **2000**, *287*, 1995−1997. (i) Liu, F.; Pak, E. B.; Singh, B.; Jensen, C. M.; Goldman, A. S. *J. Am. Chem. Soc.* **1999**, *121*, 4086−4087. (j) Jones, W. D. *Science* **2000**, *287*, 1942. (k) Sen, A. *Acc. Chem. Res.* **1998**, *31*, 550. (l) Crabtree, R. H. *J. Chem. Soc., Dalton Trans.* **2001**, *19*, 2437.

10.1021/ja051532o CCC: $30.25

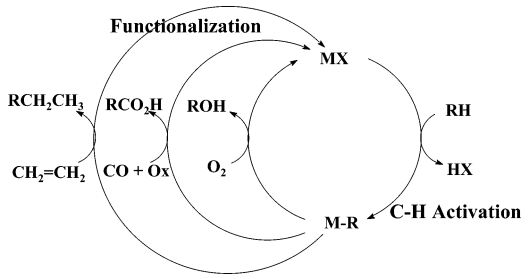

Figure 1. Catalytic cycles for generating products based on the CH activation reaction.

tion by desirable solvents, products, and reactants; (b) generating functionalized products in a catalytic sequence; and (c) stabilizing the catalysts to the conditions required for functionalization.[1h]

Complexes based on Ir are among the most active reported for the CH activation reaction.[3] We have been investigating the design of homogeneous catalysts based on Ir and other late transition metal complexes[4] using O-donor ligands such as acetylacetonate (acac),[5] tropolone,[6] aryloxides,[7] catechols,[8] hydroxyacetophenone, etc., to stabilize the complexes to the reaction conditions required for generating functionalized products. Compared to the N-, C-, or P-donor ligands generally utilized for C−H activation,[9] O-donor ligated complexes may have the potential for higher thermal, protic, and oxidant stability given the expected covalent character of oxygen−metal bonds with the late transition metals and the lower basicity of oxygen.[10]

Another key reason for study of these ligands is that the known π-donor,[11] electronegative, and "hard" characteristics of O-donor ligands could lead to electronic differences at the metal center that result in significant changes in chemistry compared to complexes based on N-, P-, and C-donors. Thus it could be anticipated that O-donor ligands might (a) facilitate access to higher oxidation states, via hard/hard interactions or π-donation during catalysis that may be required for the functionalization step shown in the generalized catalytic cycle; (Figure 1) moderate the electron density, by the interplay of σ-withdrawing and π-donating properties at the metal center, and reduce the possibility of the solvent, product, or reactant inhibition that is generally observed with very electron-rich or electron-poor metal centers; and (c) facilitate CH activation reactions with electron-rich, late transition metals that generally take place via "oxidative addition"[12] or metal insertion pathways. Recent theoretical and experimental evidence has been presented for CH activation reactions facilitated by π-donation through phenyl−Ir interactions.[13] As O-donor ligands directly attached to a metal center can be efficient π-donors,[11] it is likely that O-donor, d^6 five-coordinate, square pyramidal motifs would exhibit ground-state destabilization from nonbonding O−pπ to M−dπ, filled−filled repulsions or so-called "π-conflict"[11,14] as well as stabilization of the nonbonding O−pπ electrons by bonding interactions (or less repulsion) into the formally empty (or less filled) metal-dπ orbitals when the M−C and M−H bonds are formed by CH activation either in a transition state or as an intermediate (the metal is now formally d^4 Ir(V)), Figure 2. This stabilization is analogous the pi-donor effects of alkoxide ligands with late transition metals that facilitate binding of CO or oxidative addition to H_2 trans to the O-donor ligand as shown by Caulton.[11]

Recently, we reported a d^6 O-donor ligated Ir complex, (acac-O,O)$_2$Ir^{III}(R)(L), (acac-O,O = κ^2-O,O-acetylacetonate, L = ligand), **R**−**Ir**−**L**, (where −**Ir**− is understood to be the *trans*-(acac-O,O)$_2$Ir(III) motif throughout this paper unless specified and L is a ligand such as pyridine, Py) that shows stoichiometric and catalytic CH activation and H/D exchange of alkanes and arenes[15] as well as catalytic hydroarylation reactions with arenes.[16] Some experimental and theoretical[17] studies of this O-donor complex, **R**−**Ir**−**L**, have been reported, and a proposed mechanism for the CH activation and hydroarylation catalysis based on arene CH activation is shown in Figure 3. While O-donor ligands have been utilized with early and late transition metals,[18] to our knowledge these are the first, well-defined,

(3) (a) Arndtsen, B. A.; Bergman, R. G. *Science* **1995**, *270*, 1970. (b) Zhu, K.; Achord, P. D.; Zhang, X.; Krogh-Jespersen, K.; Goldman, A. S. *J. Am. Chem. Soc.* **2004**, *126*(40), 13044. (c) Ishiyama, T.; Takagi, J.; Hartwig, J. F.; Miyaura, N. *Angew. Chem., Int. Ed.* **2002**, *41*(16), 3056. (d) Ben-Ari, E.; Gandelman, M.; Rozenberg, H.; Shimon, L. J. W.; Milstein, D. *J. Am. Chem. Soc.* **2003**, *125*(16), 4714. Gutierrez-Puebla, E.; Monge, A.; Nicasio, M. C.; Perez, P. J.; Poveda, M. L.; Carmona, E. *Chem.−Eur. J.* **1998**, *4*(11), 2225.
(4) Liu, X. Y.; Tenn, W. J., III; Bhalla, G.; Periana, R. A. *Organometallics* **2004**, *23*, 3584−3586.
(5) Mehrotra, R. C.; Bohra, R.; Gaur, D. P. *Metal β-Diketonates and Allied Derivatives*; Academic Press: New York, 1978.
(6) (a) Muetterties, E. L.; Wright, C. M. *J. Am. Chem. Soc.* **1965**, *86*, 4706. (b) Muetterties, E. L.; Wright, C. M. *J. Am. Chem. Soc.* **1965**, *87*, 21. (c) Muetterties, E. L.; Roesky, H.; Wright, C. M. *J. Am. Chem. Soc.* **1966**, *88*, 4856. (d) Narbutt, J.; Krejzler, J. *Inorg. Chim. Acta* **1999**, *286*, 175.
(7) Bradley, D. C.; Mehrotra, R. C.; Rothwell, I. P.; Singh, A. *Alkoxo and Aryloxo Derivatives of Metals*; Academic Press: New York, 2001.
(8) (a) Pierpont, C. G.; Buchanan, R. M. *Coord. Chem. Rev.* **1981**, *38*, 45. (b) Pierpont, C. G.; Lange, C. W. *Prog. Inorg. Chem.* **1994**, *41*, 331. (c) Martin, R. *Handbook of Hydroxyacetophenones*; Kluwer: Dordrecht, The Netherlands, 1997.
(9) For example see: (a) Fulton, J. R.; Holland, A. W.; Fox, D. J.; Bergman, R. G. *Acc. Chem. Res.* **2002**, *35*, 44. (b) Jones, W. D.; Feher, F. J. *Acc. Chem. Res.* **1989**, *22*, 91. (c) Wang, C. M.; Ziller, J. W.; Flood, T. C. *J. Am. Chem. Soc.* **1995**, *117*, 1647. (e) Zhong, H. A.; Labinger, J. A.; Bercaw, J. E. *J. Am. Chem. Soc.* **2002**, *124*, 1378. (f) Johansson, L.; Ryan, O. B.; Tilset, M. *J. Am. Chem. Soc.* **1999**, *121*, 1974. (g) Fekl, U.; Goldberg, K. I. *Adv. Inorg. Chem.* **2003**, *5454*, 259. (h) Liu, F. C.; Pak, E. B.; Singh, B.; Jensen, C. M.; Goldman, A. S. *J. Am. Chem. Soc.* **1999**, *121*, 4086. (i) Nuckel, S.; Burger, P. *Angew. Chem., Int. Ed.* **2003**, *42*, 1632.
(10) (a) Bryndza, H. E.; Tam, W. *Chem. Rev.* **1988**, *88*, 1163−1188. (b) Bergman, R. G. *Polyhedon* **1995**, 3221−3237. (c) Mayer, J. M. *Polyhedron* **1995**, 3273.
(11) (a) Lunder, D. M.; Lobkovsky, E. B.; Streib, W. E.; Caulton, K. G. *J. Am. Chem. Soc.* **1991**, *113*, 1837. (b) Flood, T. C.; Lim, J. K.; Deming, M. A.; Keung, W. *Organometallics* **2000**, *19*, 1166. (c) Riehl, J.; Jean, Y.; Eisenstein, O.; Pélissier, M. *Organometallics* **1992**, *11*, 9. (d) Poulton, J. T.; Folting, K.; Streib, W. E.; Caulton, K. G. *Inorg. Chem.* **1992**, *31*, 3190.
(12) (a) Cotton, F. A.; Wilkinson, G. *Advanced Inorganic Chemistry*, 5th ed.; John Wiley & Sons: New York, 1988; pp 1189−1194. (b) Collman, J. P. *Acc. Chem. Res.* **1968**, *1*, 136 (c) Tellers, D. M.; Skoog, S. J.; Bergman, R. G.; Gunnoe, T. B.; Harman, W. D. *Organometallics* **2000**, *19*, 2428. (d) Tellers, D. M.; Bergman, R. G. *J. Am. Chem. Soc.* **2000**, *122*, 954. (e) Owen, J. S.; Labinger, J. A.; Bercaw, J. E. *J. Am. Chem. Soc.* **2004**, *126*, 8247.
(13) Krogh-Jespersen, K.; Czerw, M.; Zhu, K.; Singh, B.; Kanzelberger, M.; Darji, N.; Achord, P. D.; Renkema, K. B.; Goldman, A. S. *J. Am. Chem. Soc.* **2002**, *124*, 10797.
(14) (a) Holm, R. H. *Chem. Rev.* **1987**, *87*, 1401. (b) Bates, P. A.; Nielson, A. J.; Waters, J. M. *Polyhedron* **1987**, *6*, 163. (c) Walsh, P. J.; Hollander, F. J.; Bergman, R. G. *J. Am. Chem. Soc.* **1988**, *110*, 8729. (d) Cummins, C. C.; Baxter, S. M.; Wolczanski, P. T. *J. Am. Chem. Soc.* **1988**, *110*, 8731. (e) Parkin, G.; Bercaw, J. E. *Polyhedron* **1988**, *7*, 2053. (f) Herrmann, W. A. *Angew. Chem, Int. Ed.* **1988**, *27*, 1297. (g) Bryndza, H. E.; Domaille, P. J.; Paciello, R. A.; Bercaw, J. E. *Organometallics* **1989**, *8*, 379. (h) Chao, Y. W.; Rodgers, P. M.; Wigley, D. E.; Alexander, S. J.; Rheingold, A. L. *J. Am. Chem. Soc.* **1991**, *113*, 6326. (i) Rachidi, I. E. I.; Eisenstein, O.; Jean, Y. *New J. Chem.* **1990**, *14*, 671. (j) Caulton, K. G. *New J. Chem.* **1994**, *18*, 25.
(15) Wong-Foy, A. G.; Bhalla, G.; Liu, X. L.; Periana, R. A. *J. Am. Chem. Soc.* **2003**, *125*, 14292.
(16) (a) Periana, R. A.; Liu, X. Y.; Bhalla, G. *Chem. Commun.* **2002**, 3000. (b) Matsumoto, T.; Periana, R. A.; Taube, D. J.; Yoshida, H. *J. Mol. Catal. A: Chem.* **2002**, *180*, 1. (c) Matsumoto, T.; Periana, R. A.; Taube, D. J.; Yoshida, H. *J. Catal.* **2002**, *206*, 272. (d) Matsumoto, T.; Taube, D. J.; Periana, R. A.; Taube, H.; Yoshida, H. *J. Am. Chem. Soc.* **2000**, *122*, 7414.
(17) (a) Oxgaard, J.; Muller, R. P.; Goddard, W. A., III; Periana, R. A. *J. Am. Chem. Soc.* **2004**, *126*, 352. (b) Oxgaard, J.; Periana, R. A.; Goddard, W. A., III. *J. Am. Chem. Soc.* **2004**, *126*, 11658.

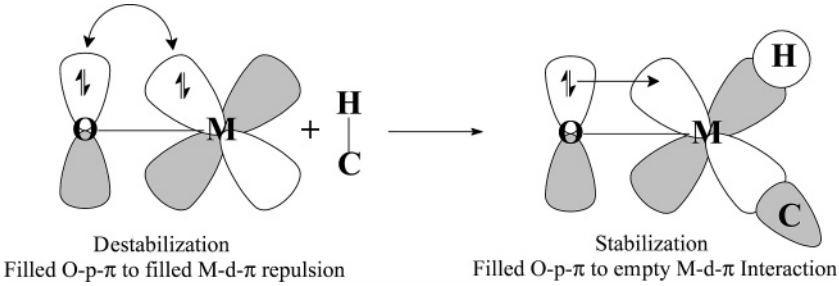

Figure 2. Schematic illustration of possible π-donor involvement of the nonbonding electrons on O-donor ligands in CH Activation reactions with oxidative addition character.

O-ligated, late transition metal complexes that activate alkane and arene C−H bonds. These late metal, O-donor complexes catalyze reactions with hydrocarbons and show significantly higher thermal stability at temperatures above 200 °C to oxidizing, acidic conditions compared to complexes based on C, N, and P ligands. Other unique characteristics are that, unlike more electron rich systems, these O-donor complexes are not severely inhibited by substrates such as olefins and water and do not generate olefinic products that would be expected from β-hydride elimination reactions.

These are intriguing characteristics and, as discussed above, may be related to the σ-acceptor and π-donor properties of the O-donor ligands. Given the potentially useful characteristics of these O-donor, bis-acac-O,O, Ir(III) complexes, we embarked on a detailed study of the stoichiometric chemistry of this class of compounds. The scope of this work includes the development of a detailed understanding of the reaction chemistry of these complexes, **R−Ir−L**, with an emphasis on providing a molecular picture of the CH activation and other reactivity of these complexes as examples of the class of late transition metal, O-donor, organometallic complexes. A particular focus of this study is to determine if the CH activation reactions of this novel class of organometallic complexes proceed by inner-sphere processes involving substrate coordination as has been found with most other systems that exhibit the CH activation reaction.[1] A desirable outcome from these studies will be to utilize this information to rationally design new, more effective, thermally protic- and oxidant-stable O-donor catalysts for hydrocarbon conversion.

2. Results and Discussion

2.1. Synthesis and Characterization of (acac-O,O)$_2$Ir(III) Complexes. The various complexes examined in this study were synthesized as shown in Scheme 1. All the complexes were fully characterized by ^{1}H, ^{13}C NMR spectroscopy, elemental analyses, and/or high-resolution mass spectrometry. In selected cases, the compounds were also characterized by X-ray crystallography. These compounds are (both aryl and alkyl, with and without β-CH bonds) stable at room temperature to air and protic solvents such as water and methanol. Importantly, the (acac-O,O)$_2$Ir(III) motif is very stable, and remarkably, refluxing complexes in acid solvents such as acetic or trifluoroacetic acids in air do not lead to loss of the acac-O,O ligands. This oxidation and protic stability is likely to arise from the octahedral geometry and the lower electropositivity at an Ir center with four electronegative O-donor ligands.

2.1.1. Dinuclear Complexes, [(acac-O,O)$_2$Ir−R]$_2$. Synthesis of the bis-acac-O,O Ir(III) complexes begins with the mononuclear bis-acac-O,O Ir(III) complex, **acac-C−Ir−H$_2$O**, that can be obtained in high yield from a modification of the procedure reported by Bennett[19] for the dinuclear complex, [Ir(μ-acac-O,O,C^3)(acac-O,O)(acac-C^3)]$_2$, **[acac-C−Ir]$_2$**. Treatment of **acac-C−Ir−H$_2$O** with ZnR_2 or HgR_2 (R = alkyl = CH_3, CH_3CH_2, and $PhCH_2CH_2$) (Scheme 1) leads to the corresponding dinuclear bis-acac-O,O iridium organometallic complexes **[R−Ir]$_2$**, in high isolated yields. For example, treatment of **acac-C−Ir−H$_2$O** in THF with $Zn(CH_3)_2$ leads to the formation of the dinuclear complex, [Ir(μ-acac-O,O,C^3)(acac-O,O)(CH$_3$)]$_2$, **[CH$_3$−Ir]$_2$** in 75% yield. The characteristic bridging acac ligands in these dinuclear iridum complexes is a common feature of these β-diketonate complexes.[20]

2.1.2. Mononuclear Complexes, (acac-O,O)$_2$Ir(R)(L). The mononuclear complexes **R−Ir−Py** can be obtained from the corresponding dinuclear complexes, **[R−Ir]$_2$** by treatment with pyridine or, in the case, of R = acac-C and R = Ph by treatment of the **acac-C−Ir−H$_2$O** with Py or Ph_2Hg followed by Py, respectively. The reactions of the dinuclear alkyl complexes **[R−Ir]$_2$**, (R = CH_3), (R = CH_2CH_2Ph) and (R = CH_2CH_3), with pyridine result in the quantitative formation of the corresponding mononuclear complex, **R−Ir−Py**. The yellow pyridine complexes **CH$_3$−Ir−Py**, **Ph−Ir−Py**, **PhCH$_2$CH$_2$−Ir−Py**, and **CH$_3$CH$_2$−Ir−Py** were all characterized by ^{1}H and ^{13}C NMR spectroscopy, elemental analysis, FAB mass spectrometry, and, in selected cases, single-crystal X-ray crystallography. ^{1}H and ^{13}C NMR spectra of these complexes are consistent with a trans-octahedral geometry. In no cases were any *cis*-(acac-O,O)$_2$Ir(R)(L) complexes isolated in these preparations. FAB mass spectral analyses of **CH$_3$−Ir−Py**,

(18) (a) Griffith, W. P. *Coord. Chem. Rev.* **1970**, *5*, 459. (b) Besecker, C. J.; Day, V. W.; Klemperer, W. G. *Organometallics* **1985**, *4*, 564. (c) LaPointe, R. E.; Wolczanski, P. T.; Van Duyne, G. D. *Organometallics* **1985**, *4*, 1810. (d) Grim, S. O.; Sangokoya, S. A.; Colquhoun, I. J.; McFarlane, W.; Khanna, R. K. *Inorg. Chem.* **1986**, *25*, 2699. (e) Klaeui, W.; Muller, A.; Eberspech, W.; Boese, R.; Goldberg, I. *J. Am. Chem. Soc.* **1987**, *109*, 164. (f) Burk, M. J.; Crabtree, R. H. *J. Am. Chem. Soc.* **1987**, *109*, 8025. (g) Burk, M. J.; Crabtree, R. H. *J. Am. Chem. Soc.* **1987**, *109*, 8025. (h) Fryzuk, M. D.; Montgomery, C. D. *Coord. Chem. Rev.* **1989**, *95*, 1. (i) Power, P. P.; *Comments Inorg. Chem.* **1989**, *8*, 177. (j) West, B. O. *Polyhedron* **1989**, *8*, 219. (k) Tanke, R. S.; Crabtree, R. H. *J. Am. Chem. Soc.* **1990**, *112*, 7984. (l) Lunder, D. M.; Lobkovsky, E. B.; Streib, W. E.; Caulton, K. G. *J. Am. Chem. Soc.* **1991**, *113*, 1837. (m) Poulton, J. T.; Folting, K.; Streib, W. E.; Caulton, K. G. *Inorg. Chem.* **1992**, *31*, 3190. (n) Johnson, T. T.; Huffman, J. C.; Caulton, K. G. *J. Am. Chem. Soc.* **1992**, *114*, 2725. (o) Wigley, D. E. *Prog. Inorg. Chem.* **1994**, *42*, 239. (p) Sharp, P. R. *J. Chem. Soc., Dalton Trans.* **2000**, 2647. (q) Cinellu, M. A.; Minghetti, G. *Gold Bull.* **2002**, *35*, 11.

(19) Bennett, M. A.; Mitchell, T. R. B. *Inorg. Chem.* **1976**, *15*, 2936.

(20) (a) Swallaw, A. G.; Truter, M. R. *Proc. R. Soc. London* **1960**, *A252*, 205. (b) Ingrosso, G.; Irnrnirzi, A.; Porri, L. *J. Organomet. Chem.* **1973**, *60*, C35.

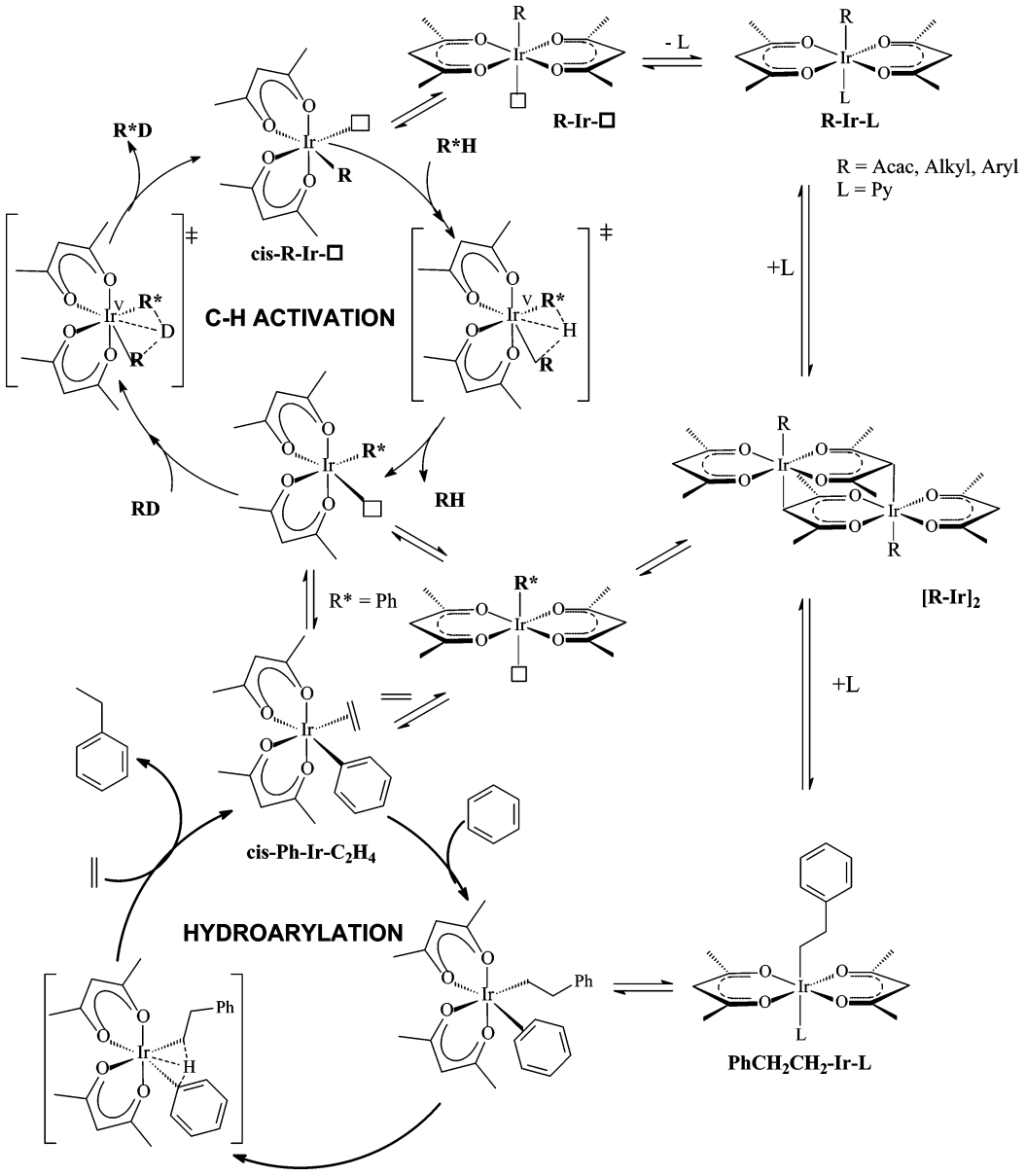

Figure 3. Proposed reaction mechanism of H/D exchange and hydroarylation of olefins catalyzed via arene C−H activation by **R−Ir−L** and **[R−Ir]$_2$** Complexes.

Ph−Ir−Py, **PhCH$_2$CH$_2$−Ir−Py**, and **CH$_3$CH$_2$−Ir−Py** show an M^+ ion of appreciable intensity. Generally, the most intense fragment is derived from the loss of the pyridine, $[M-Py]^+$. These complexes show a general trend of ion peaks for the loss of Py and the hydrocarbyl substituent, i.e., $[M^+]$, $[M-Py]^+$, and $[M-Py-R]^+$. For instance, the **Ph−Ir−Py** complex shows *m*/*z* 547.1, 468.1, and 391.1 which correspond to $[M^+]$, $[M-Py]^+$, and $[M-Py-Ph]^+$, respectively.

X-ray crystallography of selected complexes was carried out to confirm the structure of these complexes. The ORTEP projections of **Ph−Ir−Py** and **PhCH$_2$CH$_2$−Ir−Py** are shown in Figures 4 and 5, respectively.

2.2. Dynamic Behavior of Dinuclear Complexes, [(acac-O,O)$_2$Ir−R]$_2$. As communicated earlier, both the mononuclear and dinuclear (acac-O,O)$_2$Ir(III) complexes are active catalysts for C−H activation and olefin hydroarylation with anti-Markovnikov selectivity.[16] There is precedent for catalysis by dinuclear complexes with possible cooperativity between the metal centers.[21] However, given the expected strong trans influence and the weakened Ir(μ-acac-O,O,C^3) bridging bond in the **[R−Ir]$_2$** dinuclear complexes (where R is alkyl), we anticipated that reactions would be initiated by facile dissociation to generate mononuclear, coordinatively unsaturated, five-coordinate, square pyramidal intermediates, **R−Ir−□** (where □ is used as a symbol for a vacant site throughout this paper). Mechanisms involving C−H activation[1h] and olefin insertion[22] are typically inner-sphere, coordination reactions that generally require a vacant coordination site on the metal for coordination of the CH substrate, and substantial evidence can be cited for a dissociative mechanism for octahedral complexes, especially for those of Ir(III).[23] Consistent with these considerations and the observed catalytic activity of these dinuclear complexes for

(21) (a) Fryzuk, M. D.; Jones, T.; Einstein, F. W. B. *Organometallics* **1984**, *3*, 185. (b) Burch, R. R.; Shusterman, A. J.; Muetterties, E. L.; Teller, R. G.; Williams, J. M. *J. Am. Chem. Soc*. **1983**, *105*, 3546.
(22) Crabtree, R. H. *The Organometallic chemistry of the Transition Metals*, 3rd ed.; John Wiley & Sons: 2001; p 174.

Scheme 1. Synthesis of Family of O-Donor, Bis-acac Ir(III) Complexes

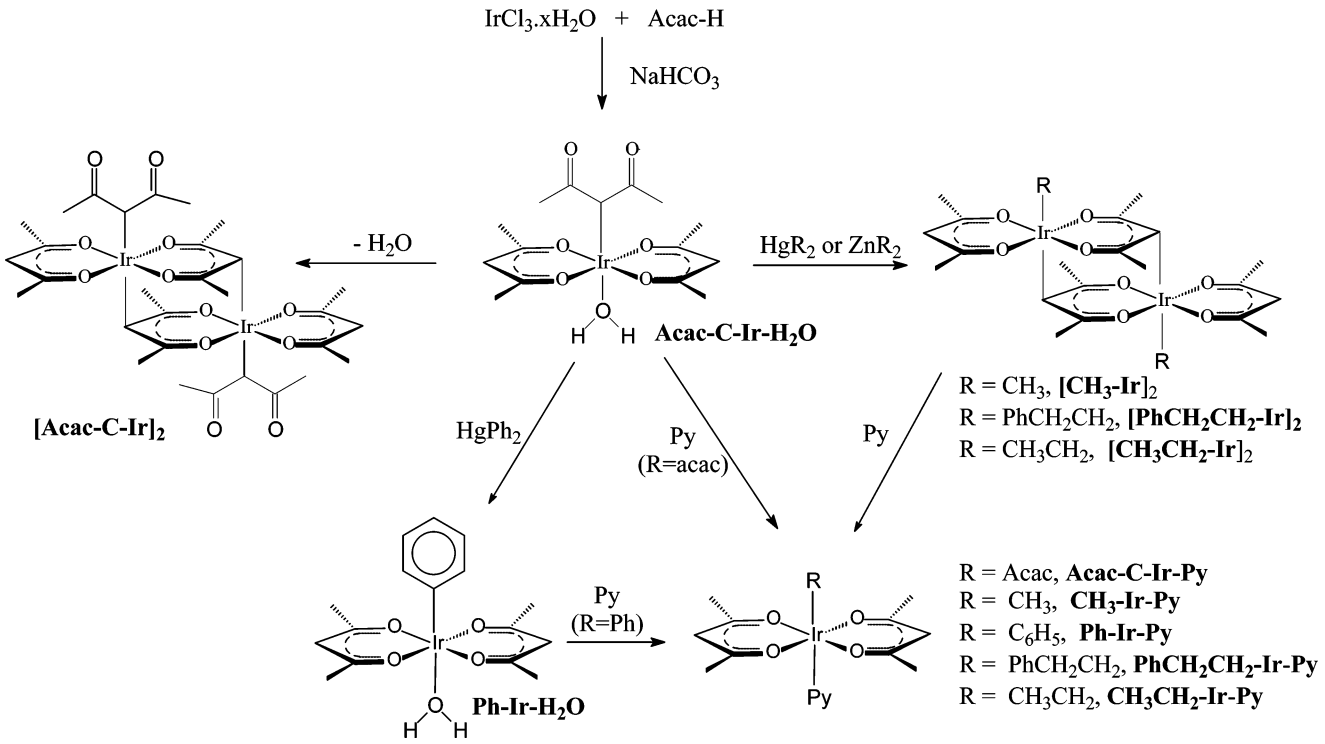

the hydroarylation reaction and catalytic H/D exchange,[16] we find the stability of the dinuclear complexes is highly dependent on the nature of the R group. For example, dinuclear complexes with electron-withdrawing groups such as chloro,[16c] **[Cl−Ir]$_2$**, or acac-C, **[acac-C−Ir]$_2$**, are stable at room temperature and show well-defined ^{1}H NMR resonances for two pairs of methyls

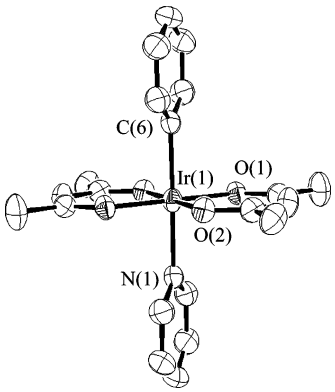

Figure 4. ORTEP diagram of complex **Ph−Ir−Py**. Selected bond angles (deg): C(6)−Ir(1)−N(1), 180.0; O(1)−Ir(1)−O(2), 95.44(18); O(2)−Ir(1)−N(1), 90.1(2); C(4)−O(2)−Ir(1), 120.7(4).

(12 H's each) and two methines (2 H's each). However, dinuclear complexes with more electron donating alkyl groups, such as **[CH$_3$−Ir]$_2$**, **[CH$_3$CH$_2$Ph−Ir]$_2$**, and **[CH$_3$CH$_2$−Ir]$_2$**, are only stable below room temperature and show dynamic behavior by NMR at room temperature that can be best explained by facile formation of the coordinatively unsaturated, five-coordinate intermediates, **R−Ir−□**, as shown in eq 1. It is possible these intermediates could be six-coordinate, solvento

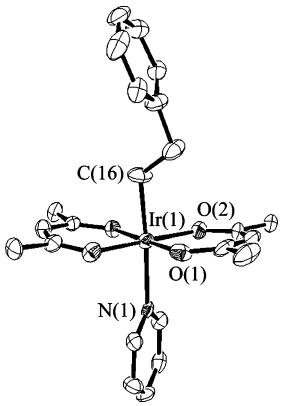

Figure 5. ORTEP diagram of complex **PhCH$_2$CH$_2$−Ir−Py**. Selected bond lengths (Å) and angles (deg): Ir(1)−C(16), 1.956(13); Ir(1)−N(1), 2.165-(7); C(16)−Ir(1)−O(1), 91.7(4); C(16)−Ir(1)−N(1), 176.5(4); O(1)−Ir(1)−N(1), 90.4(3).

complexes, but as will be discussed later, this is not consistent with the chemistry of these complexes.

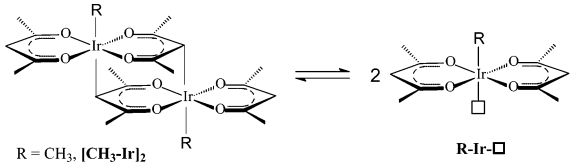

Eq. 1

The ^{1}H NMR resonances of the methyl and methine groups in the acac-O,O ligands of the dinuclear complex, **[CH$_3$−Ir]$_2$**, in tol-d_8 are broad peaks (1.8 and 5.1 ppm, respectively) at room

(23) (a) Basolo, F.; Pearson, R. G. *Mechanisms of Inorganic Reactions*; John Wiley: New York, 1968. (b) Wilkins, R. G. *The Study of Kinetics and Mechanisms of Transition Metal Complexes*; Allyn and Bacon: Boston, MA., 1974. (c) Langford, C. H.; Gray, H. B. *Ligand Substitution Processes*; W. A. Benjamin: New York, 1965. (d) Tobe, M. L. *Inorganic Reaction Mechanism*; Nelson: London, 1972. (e) Atwood, J. D. *Inorganic and Organometallic Reaction Mechanisms*; Brooks/Cole Publishing Co.: Monterey, CA, 1985.

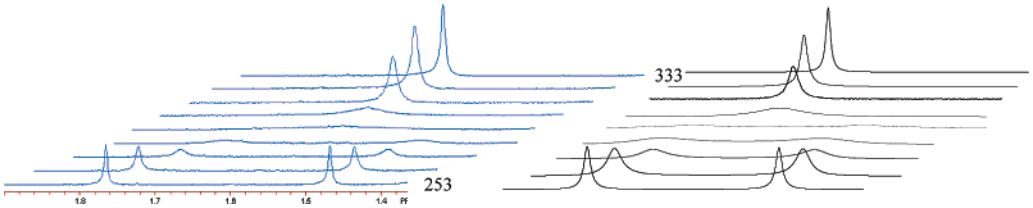

Figure 6. Variable temperature observed (left) and calculated (right) ^{1}H NMR spectra for **[CH$_3$−Ir]$_2$** in 10 K increments. Only the spectral area of interest is shown.

temperature. At lower temperatures, these signals decoalesce, and at 253 K, the NMR spectrum shows two singlets for two pairs of methyl (1.76 and 1.46 ppm, each 12 H's) and two methine resonances (5.19 and 5.02 ppm, each 2 H's) that are consistent with a stable dinuclear complex with bridging acac ligands. Similar dynamic behavior was observed for the alkyl complexes, **[PhCH$_2$CH$_2$−Ir]$_2$** and **[CH$_3$CH$_2$−Ir]$_2$**. Line broadening analysis was carried out for **[CH$_3$−Ir]$_2$** in tol-d_8 using the methyl and the methine resonances. The exchange rates were obtained in the slow-exchange region from the width of the NMR signals at half-height.[24]

The activation parameters, $\Delta H^{\ddagger} = 17.8$ ($\pm$1) kcal/mol, $\Delta S^{\ddagger} = 12.7$ ($\pm$2) eu, and $\Delta G^{\ddagger}(T = 298\ \text{K}) = 14.1$ ($\pm$0.5) kcal/mol, were derived from a linear regression analysis of the Eyring plot using rate data obtained from 253 to 333 K. A qualitative analysis was also carried out using WIND NMR, and the observed and calculated ^{1}H NMR spectra[25] of **[CH3−Ir]$_2$** are shown in Figure 6. The positive $\Delta S^{\ddagger}$ (>10 eu) value is consistent with a dissociative reaction mechanism[26] of the dinuclear complexes, **[R−Ir]$_2$** to presumably generate two coodinatively unsaturated, five-coordinate, square pyramidal species, **R−Ir−□**.

2.3. Reactions of the Dinuclear Complexes, [(acac-O,O)$_2$-Ir−R]$_2$, with Ligands. As anticipated from the proposed facile dissociation of the dinuclear complexes, these compounds react rapidly at room temperature with added ligands such as pyridine or CH$_3$OH to quantitatively generate the corresponding trans-six-coordinate, mononuclear octahedral complexes on mixing (Scheme 1). This is readily apparent by NMR analysis, as only one methyl (12 H's) resonance and one methine (2 H's) resonance are observed upon reaction of the dinuclear complexes with these ligands. While reactions of the dinuclear complexes with strong field ligands such as pyridine lead to six-coordinate monomeric species, **R−Ir−L** (L = Py), that can be isolated from solution, six-coordinate monomeric complexes formed from reaction with weak field ligands such as L = CH$_3$OH can only be observed in solution (by NMR analysis) and are not sufficiently stable to isolate without decomposition back to the dinuclear complexes.

Interestingly, attempts to generate the olefin complexes showed that olefin complexes, **R−Ir−L** (L = olefin), are also very labile. Thus, treatment of **[CH$_3$−Ir]$_2$** in tol-d_8 with 1 atm of ethylene shows no reaction by NMR, and only the broad peaks resulting from the dynamic equilibrium between the six-coordinate dinuclear and five-coordinate mononuclear complexes are observed. However, on cooling the reaction mixture to 253 K, in addition to the stable dinuclear complex, a new set of resonances consistent with a trans-six-coordinate, mononuclear olefin complex, **CH$_3$−Ir−L** (L = C$_2$H$_4$), can be observed by ^{1}H and ^{13}C NMR. Theoretical calculations show that the coordination of the ethylene only has a ΔH of −7.5 kcal/mol, indicating that the magnitude of the ΔS term will control whether the five- or six-coordinate species forms, with increased temperature drastically favoring the five-coordinate complex.

Consistent with the importance of the trans-effect, treatment of the dinuclear complexes with the weaker trans-effect acac-C ligand, **[acac-C−Ir]$_2$**, in CDCl$_3$ with ethylene (2−10 atm) at room temperature does lead to the formation of a stable, trans-six-coordinate, mononuclear, octahedral complex that could be assigned to **acac-C−Ir−C$_2$H$_4$**. However, as in the case of **CH$_3$−Ir−C$_2$H$_4$**, all attempts at isolation were unsuccessful, presumably due to facile loss of ethylene. This lack of formation of stable olefinic complexes is in stark contrast to more electron-rich complexes such as those based on more electron-rich Ir(III) complexes with Cp or phosphine ligands that readily form stable olefinic complexes.

While the ease of formation of coordinatively unsaturated intermediates in these dinuclear and mononuclear complexes may be largely due to the strong trans-effect of the strong-field alkyl groups on the stability of the Ir−C$_2$H$_4$ bond or the bridging acac, it is possible that this may also be due to the so-called "cis-effect" resulting from the lone pair effects on the O-ligands.[11,27] This effect, whereby π-donor ligands can labilize cis-groups, is presumed to operate by donation of the nonbonding π-electrons into the empty metal orbital remaining after dissociation of ligands cis to the π-donor. Since the generation of coordinative unsaturation is critical to coordination catalysis, this could be an important characteristic of O-donor ligands and we are exploring the magnitude and scope of this possibility.

2.4. Ligand (L) Substitution Chemistry of (acac-O,O)$_2$Ir-(R)(L) Complexes. Pyridine exchange in the mononuclear complexes, **R−Ir−Py**, where R is alkyl or phenyl, is quite facile at room temperature. As expected on the basis of the trans-effect and the previous bond length data, the alkyl complexes are significantly more labile than the aryl analogues. Addition of 5 equiv of Py-d_5 to a CDCl$_3$ solution of **Ph−Ir−Py** or **CH$_3$−Ir−Py** at room temperature leads to rapid Py exchange and formation of **Ph−Ir−Py-d_5** or **CH$_3$−Ir−Py-d_5** on mixing, as shown in eq 2. At low temperatures, the rate of exchange is

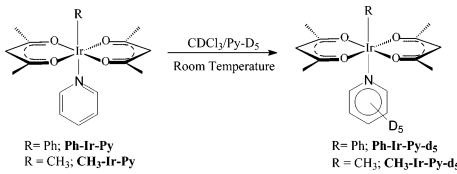

Eq. 2

(24) Günther, H. *NMR Spectroscopy*, 2nd ed.; John Wiley & Sons Limited: West Sussex, England, 1995; pp 335−346.
(25) NMR spectrum calculations were carried out using WINDNMR 7.1.6. Author: Hans J. Reich, Department of Chemistry, Wisconsin.
(26) Atwood, J. D. *Inorganic and Organometallic Reaction Mechanisms*; Wiley-VCH: New York, 1997; p 13.

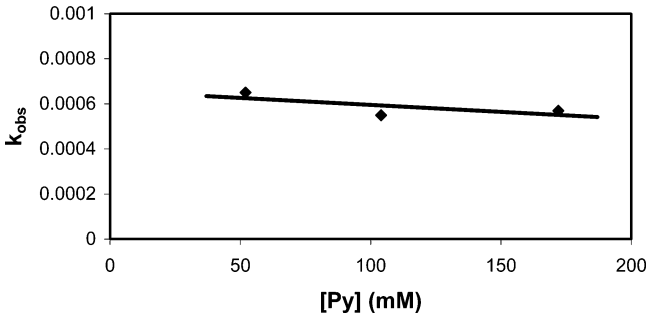

Figure 7. Plot of k_{obs} versus [Py] for pyridine exchange with **Ph−Ir−Py**.

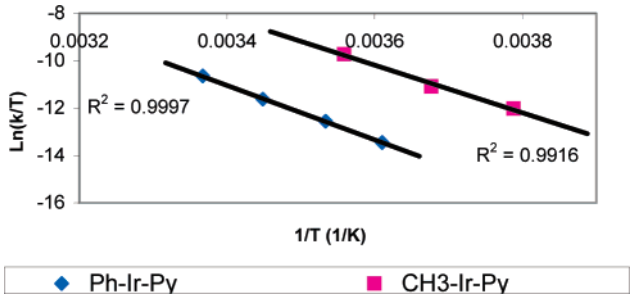

Figure 8. Eyring plot for pyridine exchange with **Ph−Ir−Py** and **CH_3−Ir−Py**.

sufficiently slow on the NMR time scale to allow the reaction kinetics to be followed from the generation of free Py-H_5 at various concentrations of Py-d_5 (under pseudo first order conditions). Kinetic studies, Figure 7, show that the reaction rate is essentially independent of added excess pyridine (52−172 mM) for **Ph−Ir−Py** as expected for a dissociative process from an octahedral Ir(III) complex. The activation parameters for the rate of exchange for **Ph−Ir−Py** were estimated to be $\Delta H^{\ddagger} = 22.8 \pm 0.5$ kcal/mol; $\Delta S^{\ddagger} = 8.4 \pm 1.6$ eu; and $\Delta G^{\ddagger}_{298K} = 20.3 \pm 1.0$ kcal/mol, Figure 8. The pyridine exchange for **CH_3−Ir−Py** was similarly found to be dissociative, with activation parameters of $\Delta H^{\ddagger} = 19.9 \pm 1.4$ kcal/mol; $\Delta S^{\ddagger} = 4.4 \pm 5.5$ eu; and $\Delta G^{\ddagger}_{298K} = 18.6 \pm 0.5$ kcal/mol, Figure 8. The previously reported values of $\Delta H^{\ddagger}$ calculated by DFT methods[17] for the loss of Py from **Ph−Ir−Py** (20.1 kcal/mol) and **CH_3−Ir−Py** (17.3 kcal/mol) to generate the coordinatively unsaturated, five-coordinate, square pyramidal complexes, **R−Ir−□** are consistent with these experimental values. The generation of these five-coordinate intermediates from the **R−Ir−Py** complexes by loss of Py is more unfavorable than in the case of the dinuclear complexes, and no dynamic behavior is observed by NMR below 100 °C. These facile exchange reactions of Ir(III), octahedral complexes are unusual, although not unique,[28] and, as discussed above, are likely due to the combination of the trans-influence of the hydrocarbyl group on the pyridine and the π-donor, O-ligands cis to the Py.

2.5. Trans−Cis Isomerization of (acac-O,O)$_2$Ir(R)(Py). As discussed above, the (acac)$_2$Ir(R)(L) complexes are typically synthesized and isolated only as the trans isomer, and it is this isomer that is utilized in these studies. However, a central premise in the proposed reaction mechanism for hydroarylation and H/D exchange is that the *trans*-(acac-O,O)$_2$Ir(R)(L) complexes are capable of isomerization to a cis-configuration that is required for both the olefin insertion and CH activation steps as seen in Figure 3. Related rearrangement has been shown for tris-acac complexes,[29] but no data was available on the barriers for such rearrangements with the bis-acac-O,O Ir(III) complexes used in the catalytic studies. Earlier theoretical calculations[17] predicted that the ***cis*-Ph−Ir−Py** complex should be *more* stable than the ***trans*-Ph−Ir−Py** isomer (by ~3 kcal/mol) and that the calculated barrier to trans−cis isomerization ($\Delta H^{\ddagger} = 42.0$ kcal/mol for **Ph−Ir−Py**) should be sufficiently high as to preclude the observation of this isomerization at room temperature and typical temperatures and reaction times employed during synthesis.

To show feasibility for the trans−cis isomerization, we investigated the conditions required to generate the ***cis*-Ph−Ir−Py** complex from the trans complex, **Ph−Ir−Py**, eq 3. The reactions were carried out in medium-pressure NMR

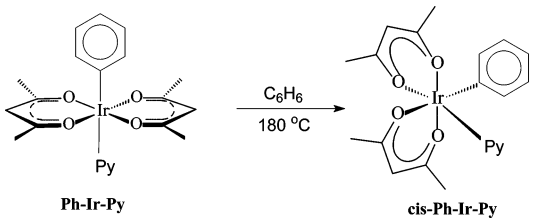

Eq. 3

tubes (with added Ar as an inert gas to prevent solvent refluxing) at 180 °C. To avoid issues of CH activation reactions of the solvent, we examined the reaction of trans-complex, **Ph-d_5−Ir−Py**, in C_6D_6 where the reactions with the solvent would be kinetically silent. The reaction progress was monitored by ^{1}H resonances of the methyl groups of the acac-O,O ligands in the starting trans-complex, **Ph−Ir−Py**, which appear as one peak that integrates to 12 protons relative to two methine protons. Importantly, control experiments showed that conversion of the trans-complex, **Ph−Ir−Py** to the deuterated trans-complex, **Ph-d_5−Ir−Py**, which is rapid in C_6D_6, does not change these methyl-acac-O,O resonances. However, as the trans−cis isomerization destroys the C_{2v} symmetry of the molecule, the formation of the cis-complex should be readily evident from the observation of four new methyl and two new methine resonances in the ^{1}H NMR.

Importantly, we find that the trans−cis isomerization proceeds cleanly and quantitatively (by NMR analysis) on heating the **Ph−Ir−Py** complex to 180 °C for 12 h. This shows that, consistent with the theoretical predictions, the ***cis*-Ph−Ir−Py** is more stable than the **Ph−Ir−Py**. To isolate and identify the cis isomer, the reaction was carried out on a preparative scale in C_6H_6. The isolated ***cis*-Ph−Ir−Py** complex has been fully characterized by ^{1}H and ^{13}C NMR spectroscopy and elemental analysis. ^{1}H and ^{13}C NMR spectra of the complex are consistent with cis-octahedral geometry.

2.5.1. Mechanism of Trans−Cis Isomerization of (acac-O,O)$_2$Ir(R)(Py). Given the central importance of this trans−cis isomerization in the CH activation and hydroarylation catalysis of these complexes, we examined the isomerization

(27) (a) Jordon, R. B. *Reaction Mechanisms of Inorganic and Organometallic Systems*; Oxford University Press: New York, 1998. (b) Davy, R. D.; Hall, M. B. *Inorg. Chem.* **1989**, *28*, 3524. (c) Flood, T. C.; Lim, J. K. Deming, M. A. *Organometallics* **2000**, *19*, 2310.

(28) Rüba, E.; Simanko, W.; Mereiter, K.; Schmid, R.; Kirchner, K. *Inorg. Chem.* **2000**, *39*, 382.

(29) Fay, R. C.; Amal, Y. G.; Klabunde, U. *J. Am. Chem. Soc.* **1970**, *92*, 7056.

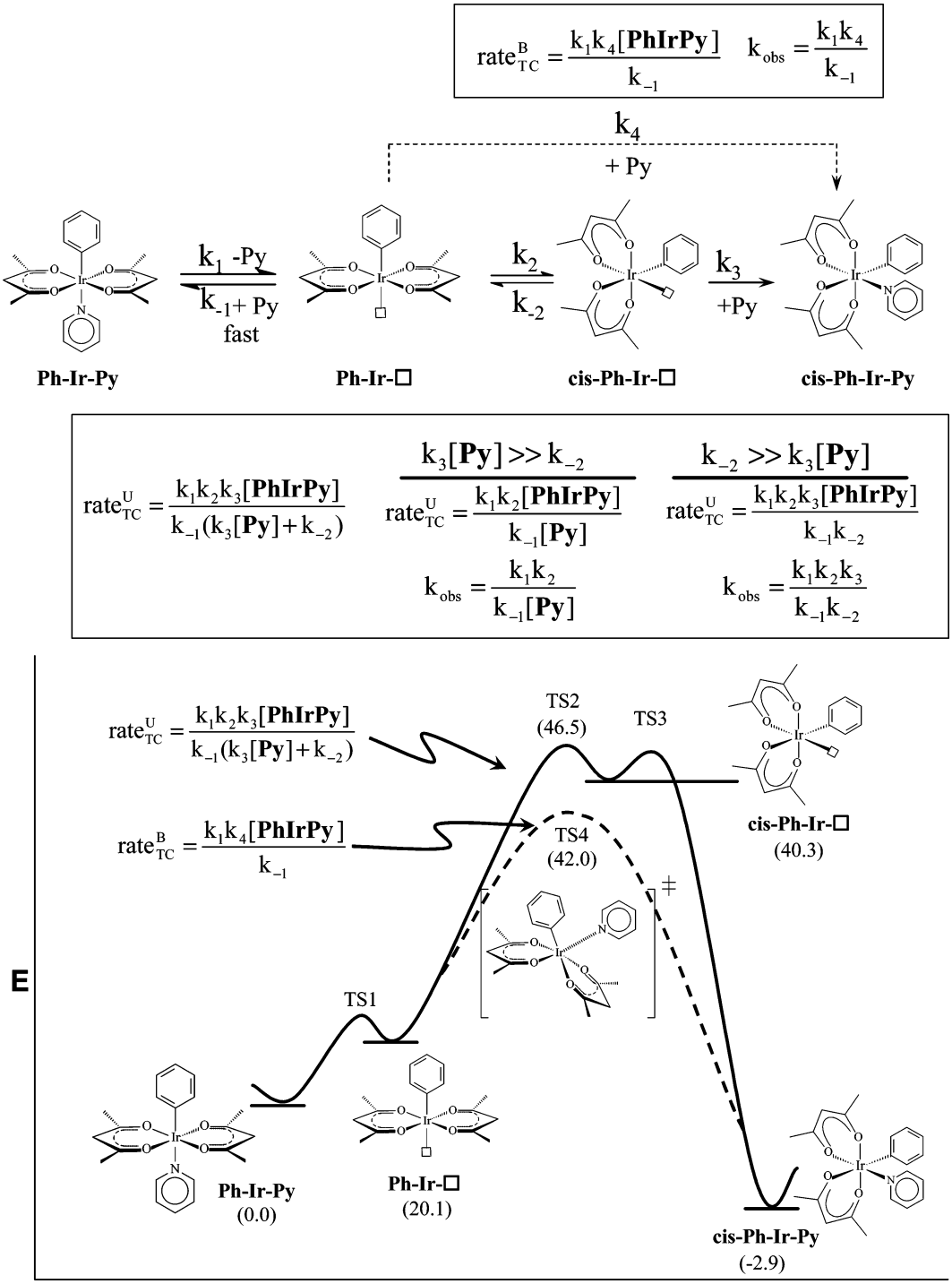

Figure 9. Possible unimolecular (U) and bimolecular (B) mechanism for trans−cis (TC) isomerization of **Ph−Ir−Py**. Predicted rate laws for trans−cis isomerization via the dissociative (solid line) and associative (dashed line) mechanisms are shown along with calculated enthalpies in parentheses.

of the **Ph−Ir−Py** complex in greater detail. In our previous theoretical study of this process,[17] two mechanisms were found to be competitive in a study of the olefin complexes, **R−Ir−Ol** (Ol = olefin); a dissociative mechanism, where trans−cis isomerization occurs with a monomolecular transition state and an associative mechanism, where the trans−cis isomerization is facilitated by coordination of olefin. The first of these related mechanisms for the isomerization of the **Ph−Ir−Py** complex is shown in Figure 9 (solid line). In this mechanism, the five-coordinate, square pyramidal intermediate, **Ph−Ir−□**, generated by reversible, dissociative loss of pyridine, undergoes a unimolecular (U), trans−cis isomerization to generate a five-coordinate cis-intermediate, ***cis*-Ph−Ir−□**, that reacts with free pyridine to generate ***cis*-Ph−Ir−Py** (TS1 → TS2 → TS3). An alternative is a direct, bimolecular (B), associative reaction of free pyridine with the five-coordinate trans-complex, **Ph−Ir−□**, to directly generate the ***cis*-Ph−Ir−Py** (TS1 → TS4).

The predicted rate laws for the two possibilities are shown in Figure 9 (using a pre-equilibrium treatment for the trans-

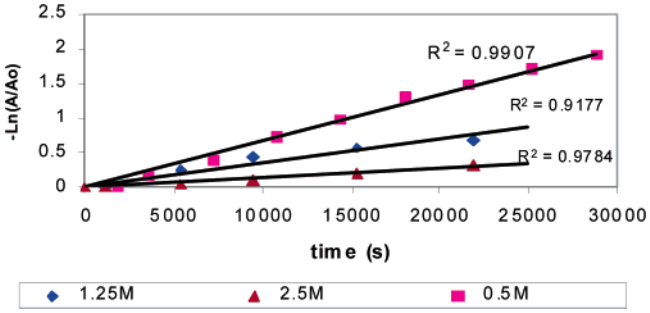

Figure 10. First-order plots for trans−cis isomerization of **Ph−Ir−Py**.

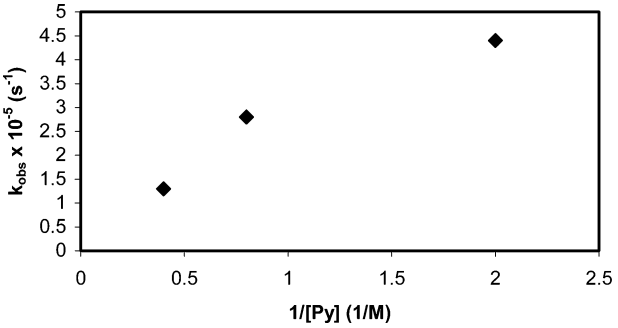

Figure 11. Plot of k_{obs} vs 1/[**Py**] for trans−cis isomerization of **Ph−Ir−Py**.

intermediate, **Ph−Ir−□**, and a steady-state approximation for the cis-intermediate, ***cis*-Ph−Ir−□**). As can be seen, only one set of conditions, via the pathway involving a unimolecular, trans−cis isomerization of **Ph−Ir−□** (TS1 → TS2 → TS3) when the formation of the five-coordinate ***cis*-Ph−Ir−□** intermediate is rate-determining (k_3[Py] > > k_{-2}), leads to a predicted inverse dependence of the k_{obs} on added pyridine. If the formation of the ***cis*-Ph−Ir−□** is slow but reversible (k_{-2} > > k_3[Py]) or if the bimolecular pathway (TS1 → TS4) is followed, the reaction rate should be independent of added pyridine. The experimental results are shown in Figures 10 and 11. As can be seen, the rate of isomerization of **Ph−Ir−Py** to ***cis*-Ph−Ir−Py** in benzene at 180 °C shows an *inverse dependence* on added pyridine over a range of 10 to 60 equiv and is consistent with trans−cis isomerization following the unimolecular pathway (TS1 → TS2 → TS3, Figure 9) involving the rate-determining formation of the five-coordinate intermediate, ***cis*-Ph−Ir−□**. As can be seen from the rate law, it is possible that at very low concentrations of pyridine, k_{-2} > > k_3[Py], reaction via ***cis*-Ph−Ir−□** could also be expected to be independent of pyridine as under these conditions it is plausible that the unimolecular isomerization of ***cis*-Ph−Ir−□** back to the trans-intermediate, **Ph−Ir−□**, would be faster than trapping by pyridine. The observation that the last data point in Figure 11 (lowest pyridine concentration) deviates significantly from a straight line through the other two points and the origin may indicate the onset of this behavior albeit three data points are not sufficient to establish this trend. Theoretical calculations also show that the barrier for reaction through TS4 is 4.5 kcal/mol lower in energy on the ΔH surface, Figure 9 (values in parentheses). However, the $T^*\Delta S$ term is expected to favor the dissociative mechanism, (assuming $\Delta\Delta S$(TS2 − TS4) ≤ 9.9 eu at 373 K) and the reaction should proceed through TS2 and largely rate-determining formation of the cis-five-coordinate intermediate, ***cis*-Ph−Ir−□**. This energy diagram would lead to the prediction that the rate of exchange of pyridine from the cis-complex, **cis-Ph−Ir−Py**, would be expected to be substantially lower than from the trans-complex since exchange of the cis-complex would require generation of ***cis*-Ph−Ir−□** which is calculated to be ∼20 kcal/mol higher than the corresponding trans-intermediate. This is indeed the case, and while the trans-complex, **Ph−Ir−Py**, exchanges with Py-d_5 on mixing at room temperature, exchange is only observed with the ***cis*-Ph−Ir−Py** above 140 °C.

These results suggest that if CH activation reactions with trans-(acac-O,O)$_2$Ir(R)(L) complexes require coordination to the cis-intermediate, ***cis*-R−Ir−□**, that the trans−cis isomerization could be expected to be an important contributor to the overall reaction rate in reactions from the trans-complexes. These results are also potentially relevant to design considerations for improved catalysts based on these trans-(acac-O,O)$_2$ Ir(III) organometallic species. Many reactions require two mutually cis sites for reaction. This geometry is typically achieved through the use of cis-tetradentate or use of tripodal ligands. An alternative strategy is to access this geometry with octahedral metal complexes having cis-bis-bidentate spectator ligands from either the cis- or trans-configurations. However, a fundamental issue with such a strategy that could lead to decreased reactivity is that the trans-configuration could be more stable than the cis and/or the barriers for isomerization can be significant. Before this study, given the known kinetic inertness of Ir complexes, we regarded this to be likely with the trans-(acac-O,O)$_2$ Ir(III) complexes and considered that the reactivity could be improved by designing cis-restricted bis-acac-O,O ligand motifs. Importantly, however, the observation that the *cis*-(acac-O,O)$_2$Ir(Ph)-(Py) complex is *more* stable than the trans-isomer now indicates that a such a strategy may *not* lead to improved rates for CH activation for this complex. Indeed, depending on the relative stability of the trans and cis bis-acac-O,O Ir(III) complexes (∼3 kcal/mol for the pyridine complexes as discussed above and comparable for the olefin complexes[17] on the basis of theoretical calculations), the cis-complexes could be less active (in the case of the pyridine complex) or comparable (in the case of the olefin complexes) assuming that TS2 and TS3 are comparable in energy. These predictions are being investigated, and preliminary results show that the rate of CH activation of benzene with ***cis*-Ph−Ir−Py** is slower than that of the corresponding trans-isomer. Thus, while the trans-isomer catalyzes H/D exchange between Tol-d_8 and C_6H_6 with a TOF of 1 × 10^{-2} s^{-1} (TN ∼50 after 2 h) at 160 °C, the ***cis*-Ph−Ir−Py** exhibits a TOF of 2 × 10^{-4} s^{-1} (TN ∼1 after 2 h) under these conditions (Figure 12). This drop in rate is consistent with the predicted ground state differences between trans and the more stable ***cis*-Ph−Ir−Py**. These results are encouraging and suggest that other readily available trans octahedral complexes with bis-bidentate spectator ligands may allow access to two mutually cis sites without significant kinetic penalty. We are currently expanding our study of other bis-bidentate octahedral metal complexes for CH activation and other reactivity studies.[30]

2.6. C−H Activation of Arenes by (acac-O,O)$_2$Ir(R)(L). 2.6.1. Rate Laws for Plausible Mechanisms of Arene CH Activation by (acac-O,O)$_2$Ir(R)(L). We define the CH activation reaction as a reaction between a CH bond and species MX

(30) Bhalla, G.; Periana, R. A. *Angew. Chem., Int. Ed.* **2005**, *44*, 1540.

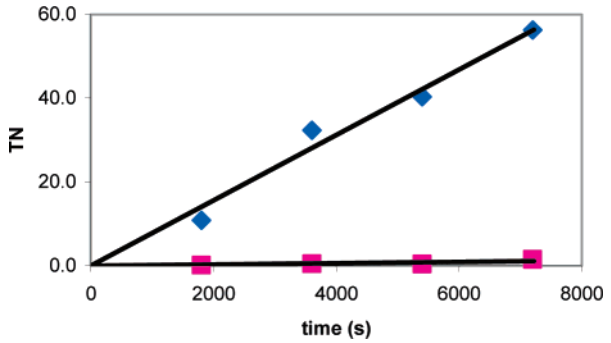

Figure 12. H−D exchange between C_6H_6 and Tol-d_8 catalyzed by **Ph−Ir−Py** (◆) and ***cis*-Ph−Ir−Py** (■) at 160 °C.

that proceeds via coordination chemistry and without the involvement of free radicals to generate M−C intermediates. As a result of the coordination characteristics of the CH activation reaction, it is generally observed to be composed of two steps: coordination of the CH bond to the metal to generate an intermediate alkane or arene complex followed by a CH cleavage step to generate the M−C intermediate.[1,3] Given the facile rate of ligand exchange with these (acac-O,O)$_2$Ir(R)(L) complexes, it is plausible that the CH activation reaction proceeds via the coordinatively unsaturated, trans-five-coordinate intermediate, **R−Ir−□**. From this intermediate two general pathways for CH activation can be considered.

One possibility is that the benzene coordination occurs before the trans−cis isomerization. In this case, benzene could react directly with the trans-intermediate, **R−Ir−□**, by coordination and CH cleavage leading to a seven-coordinate, Ir(V), intermediate or transition state that then undergoes rearrangement and loss of RH to generate the **Ph−Ir−L** product as shown in Figure 13. However, this pathway seems unlikely, as attempts at investigating this pathway by DFT calculations indicate that the intermediate or transition state resulting from CH oxidative addition trans to the R group in the trans-intermediate **R−Ir−□** could not be located, with all geometries collapsing back to **R−Ir−□**. Attempts at constraining pertinent geometry parameters such as Ir−C and/or Ir−H distances all revealed substantial energy increases on the order of >50 kcal/mol. The unfavorable CH activation with this coordinatively unsaturated trans-intermediate, **R−Ir−□**, is most likely due to a combination of two effects: (A) the destabilizing trans-effect of the R group; (B) the inflexibility of the trans acac ligands, caused by the extended aromatic system generated over the two, six-membered rings, which is necessarily perturbed if the rings are scissored away to make room for an oxidative addition.

The more likely mechanisms for the CH activation reaction from the five-coordinate, trans-intermediate, **R−Ir−□** are shown in Figure 14, involving coordination of benzene cis to the R group during the CH cleavage step. On the basis of the trans−cis isomerization studies of the **Ph−Ir−Py** complex, it could be anticipated that the most likely pathway would involve a unimolecular trans−cis isomerization of **R−Ir−□** to ***cis*-R−Ir−□**, followed by benzene coordination to generate a ***cis*-R−Ir−PhH** benzene intermediate complex, CH cleavage, and loss of RH (TS5 → TS6 → TS7 → TS8). Such a pathway is consistent with the observations that the ***cis*-Ph−Ir−Py** complex undergoes both Py exchange and CH activation at slower rates than the trans (vide infra), earlier theoretical calculations,[17] and the studies on CH activation with alkyl-Ir(III) complexes[3] that show a requirement for cis-orientation for H transfer. However, there is no requirement that cis-benzene coordination is similar to trans−cis isomerization of the **Ph−Ir−Py** complex, and pathways involving bimolecular reactions, e.g., TS9 and TS10, between benzene and **R−Ir−□** can be proposed for the CH activation as shown in Figure 14. In all cases the reaction rates are expected to show an inverse dependence on pyridine, given the low experimentally measured barrier ($\Delta G = \sim 20$ kcal/mol) for loss of pyridine from **R−Ir−Py**, while the dependence on benzene can be more complex. These dependences and other aspects of the kinetics of the CH activation reaction were examined in an attempt to distinguish between these possible pathways.

2.6.2. Products of Arene CH Activation with (acac-O,O)$_2$Ir(R)(L). As communicated earlier, these thermally protic- and oxidant-stable O-donor Ir(III) complexes readily undergo stoichiometric C−H activation of arenes and alkanes.[16] The reaction of **R−Ir−Py** with C_6D_6 at 130 °C for 1 h leads to irreversible loss of RD and quantitative formation of **Ph-d_5−Ir−Py** (based on ^{1}H and ^{13}C NMR by comparison to independently synthesized and fully characterized **Ph−Ir−Py**). This reaction is general and can be carried out with **Acac-C−Ir−Py**, **Ph−Ir−Py**, **CH$_3$−Ir−Py**, **CH$_3$CH$_2$−Ir−Py**, and **PhCH$_2$CH$_2$−Ir−Py** as shown in eq 4. Thus, when the reaction

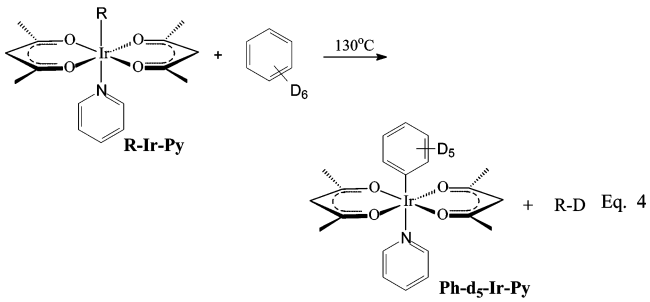

Eq. 4

of **CH$_3$−Ir−Py** is carried out in C_6D_6 at 130 °C for 1 h, the quantitative formation of CH_3D and **Ph-d_5−Ir−Py** has been confirmed by GC/MS (of the gas and liquid phase) and ^{1}H NMR spectroscopy using trimethoxybenzene as an internal standard. The higher deuterium isotopomers of methane, CH_nD_{4-n}, were not observed under the reaction conditions even after longer reaction times. This shows that the generation of methane under these conditions is essentially irreversible (at higher temperatures, reaction with methane can be observed). Indeed, theoretical calculations for the replacement of methyl for phenyl is exothermic by ~15 kcal/mol.[15,17] Similarly, heating other alkyl complexes (**PhCH$_2$CH$_2$−Ir−Py** and **CH$_3$CH$_2$−Ir−Py**) in neat C_6D_6 led to the quantitative and irreversible formation of the corresponding monodeuterated hydrocarbons, $PhCH_2CH_2D$ and CH_3CH_2D, respectively, and **Ph-d_5−Ir−Py**. In the case of reaction of **PhCH$_2$CH$_2$−Ir−Py**, only the $PhCH_2CH_2D$ regioisotopomer is formed as determined by ^{1}H NMR of the reaction products.

Interestingly, unlike the alkyl-Ir complexes, treating **Ph−Ir−Py** with tol-d_8 for short times (~20% conversion to minimize post H/D scrambling of the benzene product since this reaction is reversible) led to the formation of multiple deuterated isotopomers of benzene rather than only the monodeuterated product, C_6H_5D. This observation of multiple deuterium incorporation into the benzene eliminated from

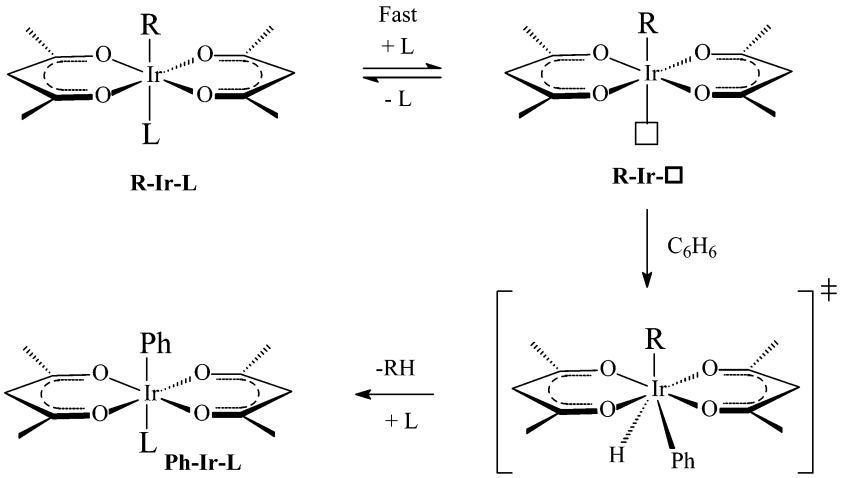

Figure 13. Possible CH activation pathway involving the trans-intermediate, **R**−**Ir**−□.

Ph−**Ir**−**Py** on treatment with tol-d_8 is characteristic of the generation of intermediate arene complexes in a rate-determining step during CH activation reactions.[31] To examine this possibility and elucidate the details of the CH activation reactions we turned to kinetic studies.

2.6.3. Activation Barrier for CH Activation using CH_3−Ir−Py. The **CH_3**−**Ir**−**Py** complex was used to obtain the barrier for arene CH activation. Due to the poor solubility of the **Ph**−**Ir**−**Py** in benzene and overlapping aromatic resonances in the ^{1}H NMR, the arene CH activation barrier with this complex could not be accurately obtained. As previous studies[16] showed that the CH activation was inhibited by added pyridine, the activation barriers were obtained at constant pyridine concentrations. The temperature dependence of the reaction was examined over the range 140−180 °C in neat C_6D_6 at a constant pyridine concentration ([Py]/[C_6D_6] = 0.045). The reaction follows clean first-order kinetics, and to determine the reaction rates, ^{1}H NMR spectroscopy of the methyl resonances of the acac-O,O ligands was used to monitor the irreversible disappearance of the **CH_3**−**Ir**−**Py** starting material and the formation of the **Ph-d_5**−**Ir**−**Py** product for three half-lives. Activation parameters were obtained from an Eyring plot as shown in Figure 15. The activation entropy ($\Delta S^{\ddagger}$) was estimated to be 11.5 (±3.0) eu along with a $\Delta H^{\ddagger}$ of 41.1 (±1.1) kcal/mol and $\Delta G^{\ddagger}_{298}$ of 37.7 (±1.0) kcal/mol. The **$PhCH_2CH_2$**−**Ir**−**Py** complex was found to react at essentially the same rates as **CH_3**−**Ir**−**Py**, and as can be seen in Figure 15, the experimentally determined rate for arene CH activation with **$PhCH_2CH_2$**−**Ir**−**Py** shows similar temperature dependence to that of **CH_3**−**Ir**−**Py**. The previously calculated CH activation barrier[17] for a pathway proceeding via a cis-intermediate was found to be ∼ 43 kcal/mol ($\Delta H^{\ddagger}$) for the **$PhCH_2CH_2$**−**Ir**−**Py** and is consistent with the value obtained in this experimental study.

2.6.4. Dependence of CH Activation on Pyridine Concentration. If the CH activation reaction proceeded, as proposed in Figure 14, from the five-coordinate trans-intermediate, **R**−**Ir**−□, then the CH activation should show an inverse dependence on added pyridine as shown in the possible rate laws. To confirm this, the rate of the C−H activation reaction of **$PhCH_2CH_2$**−**Ir**−**Py** was obtained in the presence of 15 to 44 equiv of pyridine (223 to 669 mM), Figures 16 and 17. The reactions are clean and quantitatively generate the trans-complex, **Ph-d_5**−**Ir**−**Py**. There are very little complications at these concentrations of pyridine with CH activation of the pyridine. The rate of formation of the cis-complexes (**R**−**Ir**−**Py**, R = Ph or Alkyl) is slower than the CH activation reaction at 140 °C and is not observed on the time scale of these experiments.

As can be seen, the rate of CH activation shows an inverse dependence on added pyridine. This is consistent with the CH activation reaction proceeding via the formation of the *trans*-five-coordinate complex, **$PhCH_2CH_2$**−**Ir**−□, that is formed by prior, rapid, reversible, dissociative loss of pyridine and is consistent with either rate law shown in Figure 14.

2.6.5. Arene Substrate Concentration Dependence. As can be seen in Figure 14 from the various possible mechanisms and associated rate laws for arene CH activation, there is the possibility that the reaction could show a direct dependence, independence, or more complex dependence on the benzene concentration. Both arene dependent and independent kinetics have been reported for arene for CH activation.[32,33] To begin to distinguish between these possibilities, we examined the dependence of the arene CH activation rate on the arene substrate concentration. A key challenge in carrying out such a study is to identify an inert solvent that could be used as a diluent for the benzene substrate. Due to a combination of reactivity and solubility issues, solvents such as fluoropyridine, hexafluorobenzene, or trifluoroethanol could not be utilized. Instead, we utilized a strategy of carrying out the CH activation reactions in cyclohexane-d_{12} solvent using the **Cy-d_{11}**−**Ir**−**Py** (where Cy-d_{11} is the perdeuterated cyclohexyl group), with varying amounts of added excess C_6D_6 (1600−5600 mM to ensure pseudo first-order reaction conditions). Under these conditions, any reactions with the solvent would be degenerate and kinetically silent. The reactions were followed by analyzing the loss of the **Cy-d_{11}**−**Ir**−**Py** relative to trimethoxybenzene as an internal standard at 120 °C, and the results are shown in Figure 18. The **Ph-d_5**−**Ir**−**Py** product was not completely soluble

(31) (a) Jones, W. D. *Acc. Chem. Res.* **2003**, *36*, 140. (b) Jones, W. D.; Feher, F. J. *J. Am. Chem. Soc.* **1986**, *108*, 4814−4819.

(32) (a) Tellers, D. M.; Bergman, R. G. *Can. J. Chem.* **2001**, *79*, 525−528. (b) Tellers, D. M.; Yung, C. M.; Arndtsen, B. A.; Adamson, D. R.; Bergman, R. G. *J. Am. Chem. Soc.* **2002**, *124*, 1400.

(33) (a) Johansson, L.; Tilset, M. *J. Am. Chem. Soc.* **2001**, 739. (b) Johansson, L.; Tilset, M.; Labinger, J. A.; Bercaw, J. E. *J. Am. Chem. Soc.* **2000**, 10846.

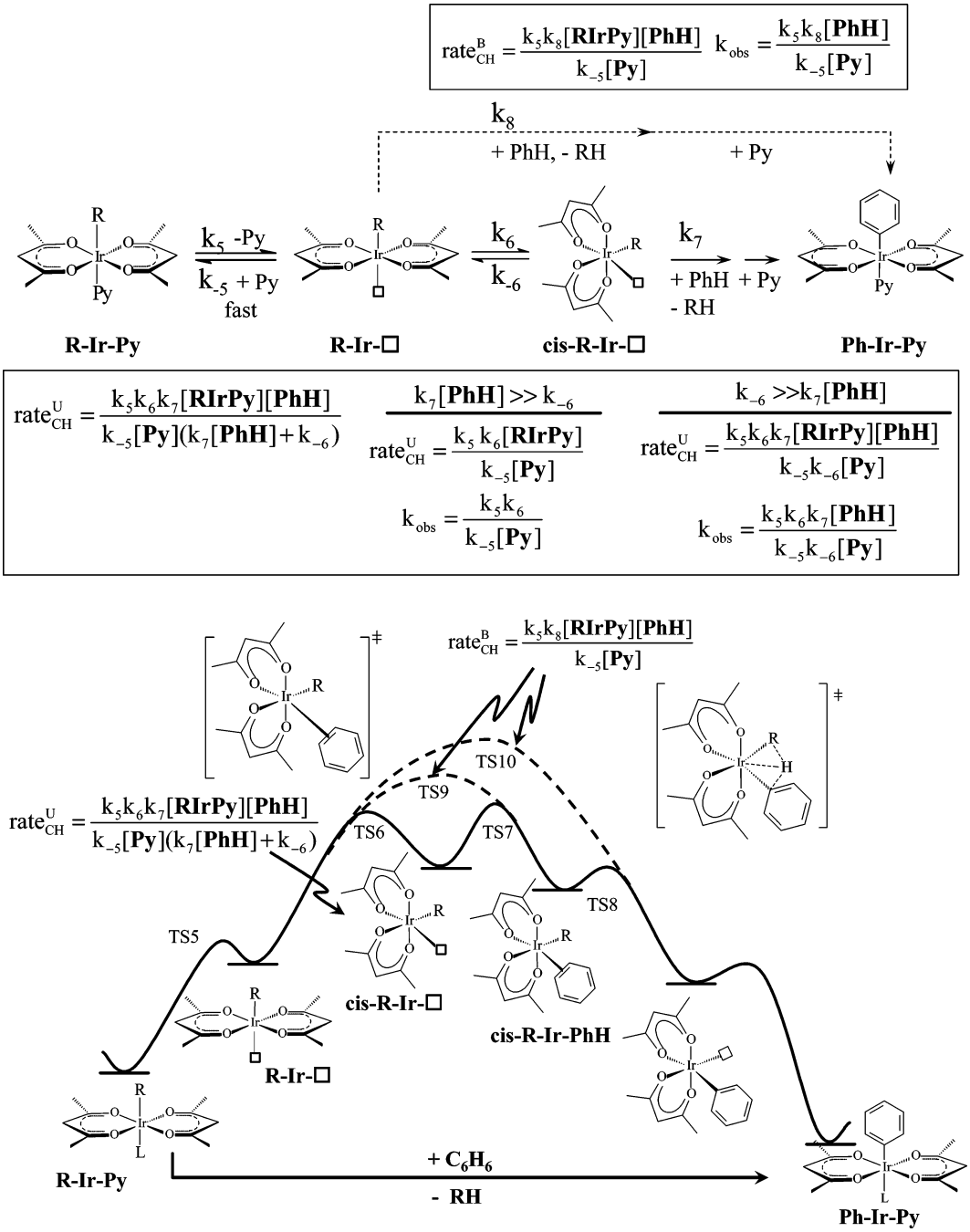

Figure 14. Possible CH activation pathways involving reaction of benzene with **R−Ir−Py** species.

under these reaction conditions, and to ensure that loss of **Cy-*d*$_{11}$−Ir−Py** resulted only from formation of **Ph-*d*$_5$−Ir−Py**, CD_2Cl_2 was added after reaction to dissolve all products and the trimethoxybenzene was used as an internal standard to ensure that **Ph-*d*$_5$−Ir−Py** produced accounted for >95% of the reacted **Cy-*d*$_{11}$−Ir−Py**. The lack of unreacted **Cy-*d*$_{11}$−Ir−Py** after long reaction times ensured that the reaction to generate **Ph-*d*$_5$−Ir−Py** was irreversible under the reaction conditions, and simple first-order plots could be used to obtain the rate constants.

As can be seen from Figure 18, the CH activation reaction shows a linear dependence on the benzene concentration that indicates that benzene is involved prior to or in the rate-determining step. This observation rules out the unimolecular possibility that k_7[PhH] > > k_{-6}, $k_{obs} = k_5k_6/k_{-5}$[Py], (Figure 14), and shows that, unlike the case with isomerization of **Ph−Ir−Py**, (at least at the concentrations of benzene examined) the formation of the cis-five-coordinate intermediate, ***cis*-R−Ir−□**, cannot be the rate-determining step and that benzene is involved in the rate-determining step for arene CH activation. Indeed, this observation does not provide any evidence for the formation of a cis-five-coordinate intermediate, ***cis*-R−Ir−□**, or indicate whether an arene complex is formed, if the CH cleavage step is rate-determining or if the CH activation reaction is concerted from the trans-five-coordinate intermediate, **R−Ir−□**. To distinguish between these possibilities, we turned to studies of the kinetic deuterium isotope effects on the CH activation reactions of **R−Ir−Py**.

2.6.6. Isotope Effects on the Rate of CH Activation with (acac-O,O)Ir(R)(L) Complexes. As discussed above, the

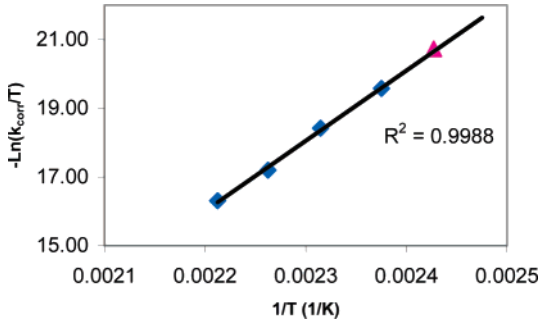

Figure 15. Eyring plot for the reaction of **CH_3−Ir−Py** (◆) with C_6D_6 at $[Py]/[C_6D_6] = 0.045$. $k_{corr} = k_{obs} \times [Py]/[C_6D_6]$. (▲) = **$PhCH_2CH_2$−Ir−Py**.

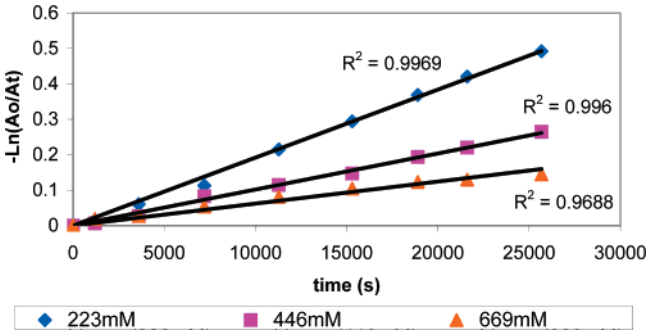

Figure 16. First-order plots for Py_{added} for C−H activation of **$PhCH_2CH_2$−Ir−Py** at 140 °C.

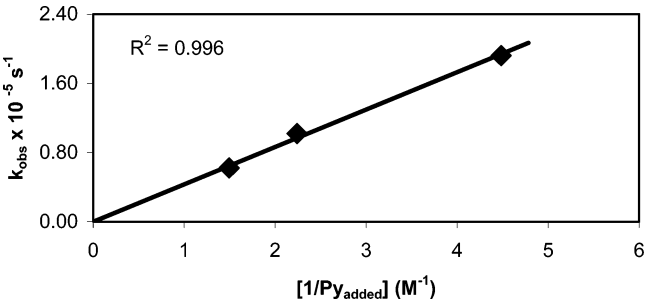

Figure 17. Plot of k_{obs} vs 1/**Py** for C−H activation of **$PhCH_2CH_2$−Ir−Py** at 140 °C.

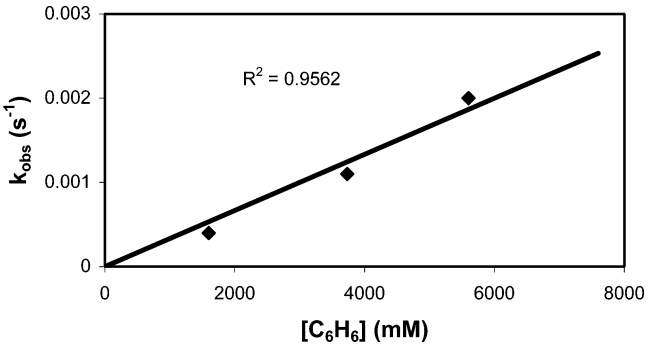

Figure 18. Plot of k_{obs} vs $[C_6H_6]$ at 120 °C with **Cy-d_{11}−Ir−Py**.

observation that the reaction of **Ph−Ir−Py** with tol-d_8 leads to multiple deuterated benzenes is most consistent with the CH activation reaction proceeding via the formation of an intermediate arene complex, followed by rapid and reversible CH cleavage before loss of the arene. To examine this possibility in greater detail, we turned to the now classic method, developed by W. Jones, of providing evidence for the intermediacy of arene complexes by comparison of the deuterium kinetic isotope effect (KIE) on the relative rates of CH activation when reactions are carried out with a mixture of C_6D_6/C_6H_6 and with 1,3,5-trideuteriobenzene.[31] Three possibilities for the CH activation of benzene with **CH_3−Ir−Py** can be considered with respect to the formation of arene complexes as shown in Figure 19: (A) a concerted process without the involvement of an arene complex (TS5 → TS10), (B) rate-determining CH cleavage proceeding via an arene complex, ***cis*-CH_3−Ir−PhH**, (TS5 → TS9 → TS11 or TS5 → TS6 → TS7 → TS11) that is kinetically indistinguishable by KIE from case A, and (C) rate-determining trans to cis isomerization and benzene coordination followed by rapid CH cleavage (TS5 → TS6 → TS7 → TS8). As can be seen if CH cleavage is rate-determining, case A or B, both the C_6D_6/C_6H_6 mixture and neat 1,3,5-$C_6D_3H_3$ will be expected to show a normal kinetic isotope effect. However, if an arene complex is formed in a rate-determining step *and* followed by faster CH cleavage (case C), *only* the reaction with 1,3,5-$C_6D_3H_3$ will show a normal KIE; the reaction with C_6D_6/C_6H_6 will show *no* KIE.

As discussed above, the reaction of **CH_3−Ir−Py** with C_6D_6 proceeds quantitatively and irreversibly to produce only CH_3D. Thus, analysis of the CH_4/CH_3D ratio produced from CH activation with **CH_3−Ir−Py** provides a convenient method of determining the KIE for CH activation with this complex. The CH activation reaction was carried out by reaction of **CH_3−Ir−Py** at 110 °C with neat 1,3,5-$C_6H_3D_3$, a 1:1 (molar) mixture of C_6H_6/C_6D_6 and neat C_6D_6 as solvents in separate reactions. In all three cases, the methane generated was analyzed by GC−MS, and the molar ratios of the methane CH_4/CH_3D isotopomers were determined by deconvolution of the mass peaks based on actual response factors and fragmentation patterns from pure samples of CH_4 and CH_3D. Since it is known that these (acac-O,O)Ir(III) complexes will catalyze H/D exchange between arenes, the reactions were carried out for three half-lives and GC−MS analysis of the various solvents after reaction confirmed that no significant extent of H/D scrambling had occurred in the $C_6D_6-C_6H_6$ mixture or 1,3,5-$C_6H_3D_3$ solvents. The results are shown in Table 1.

As discussed above, the observation that only CH_3D was produced in the reaction with neat C_6D_6 ruled out any error that could be introduced from post H−D exchange of the generated methane.[34] Control experiments in neat C_6H_6 also confirmed that only CH_4 is generated. As can be seen, no kinetic isotope effect is observed for the C_6D_6/C_6H_6 mixture since a 1:1 ratio of CH_4/CH_3D is produced. This result effectively rules out pathways via TS10 and TS11 that involve CH cleavage in the rate-determining step. The rather large kinetic isotope effect (considering the temperature of 110 °C) of 3.2 (±0.2) that is observed with 1,3,5-$C_6H_3D_3$ suggests that the reaction proceeds via TS5 → TS6 → TS7 → TS8 or TS5 → TS9 → TS8 that involve rate-determining coordination of benzene, followed by rapid CH cleavage. These results provide strong evidence that intermediate arene complexes are involved in the CH activation with the O-donor $(acac-O,O)_2Ir(R)(L)$ complexes and that CH activation with these O-donor complexes are inner-sphere processes involving substrate coordination.

2.6.7. Does the CH Activation Reaction Proceed via a cis-Five-Coordinate Intermediate? Importantly, these KIE and

(34) Methane can exchange with benzene at elevated temperatures and lead to higher isotopomers of methane as reported, ref 15.

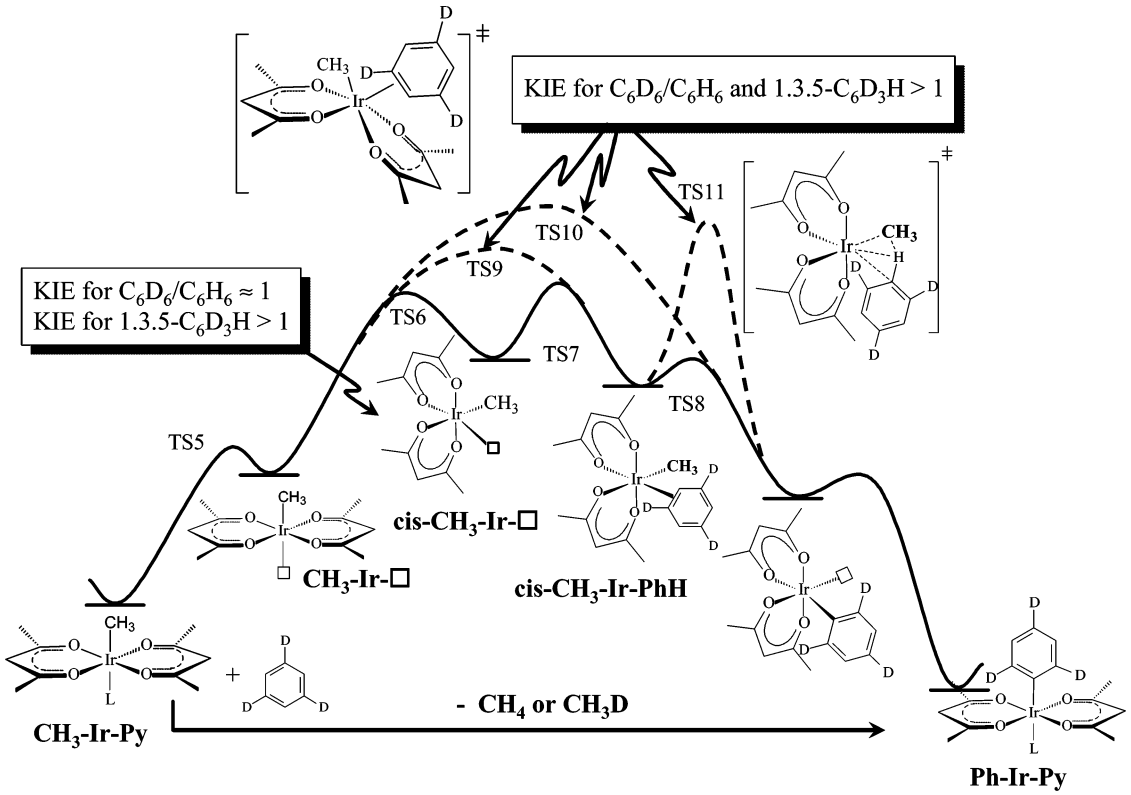

Figure 19. Possible reaction coordinate for reaction of **CH_3−Ir−Py** with 1,3,5-$C_6D_3H_3$.

Table 1. Methane Isotopomer Ratio Obtained from Reaction of **CH_3−Ir−Py** with Various Solvents

	solvents		
isotopomer[a]	C_6D_6	1,3,5-$C_6H_3D_3$	C_6H_6/C_6D_6 (1:1 molar mixture)
CH_4	0	76	50
CH_3D	100	24	50

[a] See Experimental Section for details.

kinetic studies do not address the question of whether the formation of these intermediate arene complexes are generated via the formation of the cis-five-coordinate intermediate ***cis*-R−Ir−□** (TS5 → TS6 → TS7, Figure 19), or directly, in an associative step from the trans-five-coordinate intermediate, **R−Ir−□** (TS5 → TS9, Figure 19). The trans−cis isomerization studies of the **Ph−Ir−Py** complex provide evidence for the rate-determining formation of such cis-intermediates, vide supra. Since the formation of the cis-benzene complex, ***cis*-R−Ir−PhH**, is essentially the same process as the formation of the cis-pyridine complex, ***cis*-Ph−Ir−Py**, it is likely that formation of the benzene complex also proceeds by formation of the cis-five-coordinate intermediate, ***cis*-R−Ir−□**, and that this should constitute the bulk of the barrier for the reaction with benzene. If this is the case, the rate constant for CH activation should be similar to the rate constant for the trans to cis isomerization for these complexes (obtained when the reaction rates are corrected for benzene and pyridine concentrations). This has been examined both theoretically and experimentally.

Theoretical results for the reaction of **CH_3−Ir−Py** with benzene, summarized in Figure 20, show that these rate constants should be comparable as the formation of ***cis*-R−Ir−□** is found to be the slowest step in both reactions. The cis/trans isomerization has a $\Delta H^{\ddagger} = 44.6$ kcal/mol, while CH activation has a $\Delta H^{\ddagger} = 43.4$ kcal/mol. ΔS terms are expected to be of similar magnitude, as the total number of molecules does not change.

Experimentally, the rates of the trans−cis and CH activation have been obtained under identical conditions (180 °C and pyridine to benzene ratio of 0.045) where the trans−cis isomerization shows an inverse dependence on pyridine, and the CH activation, a direct dependence on benzene. Taking the ratio of the appropriate cases of the rate laws, Figure 14, and assuming these reactions proceed via the formation of the cis-five-coordinate intermediate, Scheme 2, allow the ratio of the rate constants for the CH activation, k_{CH}, and trans−cis isomerization, k_{TC}, to be compared. As can be seen, this ratio is ∼1. It may be considered that this specific comparison is not entirely valid as different complexes, the **Ph−Ir−Py** and the **CH_3−Ir−Py**, are utilized in the trans−cis isomerization and CH activation reactions, respectively. However, extrapolation of the equilibrium constants for the loss of pyridine from **Ph−Ir−Py** and **CH_3−Ir−Py** show that at 180 °C the values are comparable, $\sim 0.7 \times 10^{-9}$ and $\sim 2.0 \times 10^{-9}$, respectively, and we anticipate that the trans−cis isomerization steps should be energetically similar for these complexes. This suggests that the comparable rate constants for these reactions are consistent with the CH activation and trans−cis reactions proceeding via a common intermediate, the cis-five-coodinate intermediate, ***cis*-R−Ir−□** and that the energetics of benzene coordination to this species, TS10 and k_7 (Figures 13 and 18), do not significantly contribute to the activation barrier for CH activation.

A comparison of the rates for trans−cis isomerization and CH activation via the ***cis*-R−Ir−□** intermediate also explains why no ***cis*-R−Ir−Py** species are detected under typical CH activation conditions with **R−Ir−Py** (∼140 °C and no added

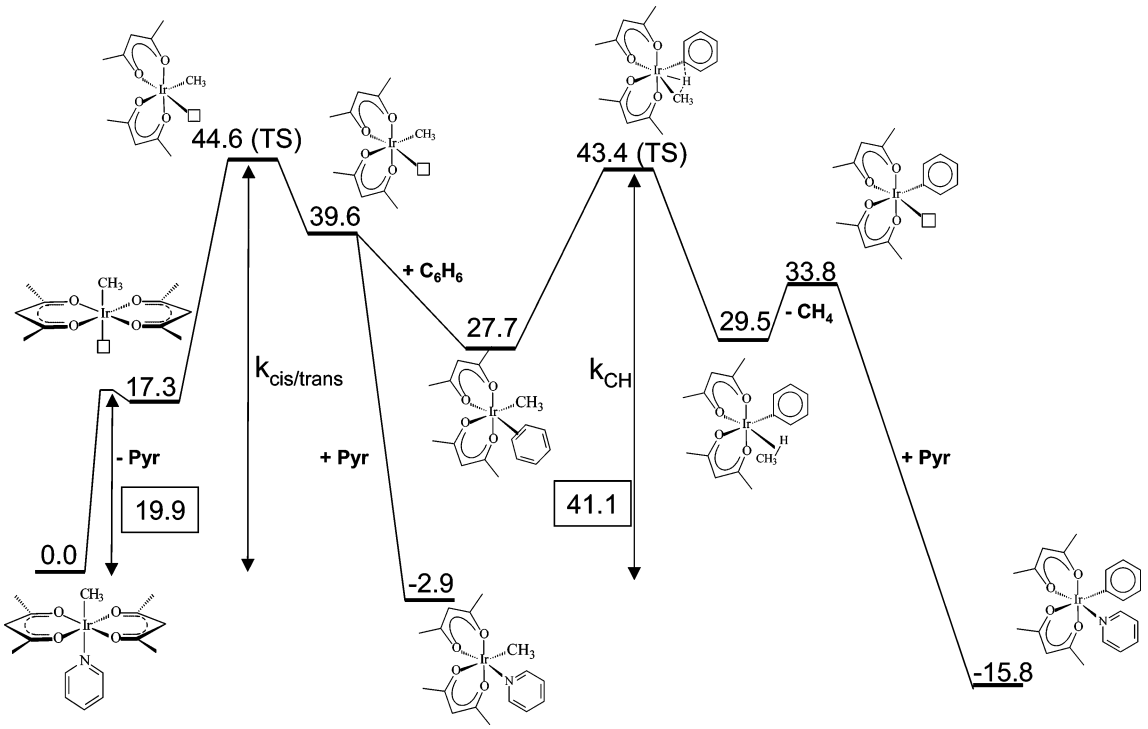

Figure 20. Theoretical calculations of trans−cis isomerization and C−H activation. Boxed values are the experimental values for that step.

Scheme 2. Ratio of Rate Laws for Isomerization and CH Activation

Rate law for CH activation ($k_{-6} >> k_7[\mathbf{PhH}]$)

$$\text{rate}^{U}_{CH} = \frac{k_{CH}[\mathbf{RIrPy}][\mathbf{PhH}]}{[\mathbf{Py}]}$$

Rate law for trans-cis isomerization ($k_3[\mathbf{Py}] >> k_{-2}$)

$$\text{rate}^{U}_{TC} = \frac{k_{TC}[\mathbf{PhIrPy}]}{[\mathbf{Py}]}$$

$$\frac{\text{rate}^{U}_{TC}}{\text{rate}^{U}_{CH}} = \frac{k_{TC}[\mathbf{PhIrPy}]}{k_{CH}[\mathbf{RIrPy}[\mathbf{PhH}]}$$

$$\frac{k_{TC}}{k_{CH}} = \frac{\text{rate}^{U}_{TC}[\text{PhH}]}{\text{rate}^{U}_{CH}} = \frac{4.5\times10^{-5}[11.2]}{8\times10^{-4}} = 0.6 \approx 1$$

Scheme 3. Ratio of Rate Laws for Isomerization and CH Activation

Rate law for CH activation ($k_{-6} >> k_7[\mathbf{PhH}]$)

$$\text{rate}^{U}_{CH} = \frac{k_{CH}[\mathbf{RIrPy}][\mathbf{PhH}]}{[\mathbf{Py}]}$$

Rate law for trans-cis isomerization ($k_{-2} >> k_3[\mathbf{Py}]$)

$$\text{rate}^{U}_{TC} = k^{*}_{TC}[\mathbf{PhIrPy}]$$

$$\frac{\text{rate}^{U}_{TC}}{\text{rate}^{U}_{CH}} = \frac{k^{*}_{TC}[\mathbf{PhIrPy}][\mathbf{Py}]}{k_{CH}[\mathbf{RIrPy}[\mathbf{PhH}]} \approx \frac{[\mathbf{Py}]}{[\mathbf{PhH}]} \approx 10^{-6}$$

Py). Under these conditions, the appropriate rate law for the trans−cis isomerization is that shown in Scheme 3, where because of the low concentration of pyridine the reaction is independent of pyridine ($k_{-2} \gg k_3$[Py], Figure 9) while the rate of CH activation remains inversely dependent on pyridine and directly dependent on benzene ($k_{-6} \ll k_7$[PhH], Figure 14). Thus, assuming that the rate constants k_{TC}* for these steps are comparable, at comparable concentrations of complexes the relative rates of trans-cis isomerization to CH activation would be given by [Py]/[PhH] which, based on the experimental equilibrium values for pyridine dissociation from **R−Ir−Py**, is $\sim 10^{-6}$. This low value is consistent with the observation that no cis-products are detected after the CH activation reaction is complete. At higher pyridine concentrations, the ratio of these rates would be expected to become comparable (as the rate law changes to those shown in Scheme 2 and both reactions become independent of added pyridine), and the trans−cis isomerization should be observed along with CH activation. This is observed experimentally, and at pyridine concentrations above 1 M, the ***cis*-Ph−Ir−Py** is observed during the CH activation of benzene with **CH_3−Ir−Py**. However, clean kinetics could not be obtained under these conditions as the reaction is complicated by CH activation of pyridine.

3. Conclusion

The chemistry of novel (acac-O,O)$_2$Ir(R)(L) organometallic complexes has been examined in detail. The dinuclear, **[R−Ir]$_2$**, as well as mononuclear complexes, **R−Ir−L**, have been found to be labile complexes that are in equilibrium, via dissociative processes, with trans-five-coordinate species, **R−Ir−□**, that are key intermediates in the substitution chemistry of these complexes. These **R−Ir−L** complexes have also been shown to undergo trans−cis isomerization via a rate-determining, unimolecular isomerization of **R−Ir−□** to ***cis*-R−Ir−□**, followed by rapid reaction with substrates. Bimolecular pathways involving direct reaction of the substrate with the trans-intermediate, **R−Ir−□**, are not consistent with the experimental or theoretical results.

Arene CH activation with these O-donor complexes has been shown to occur via an inner-sphere process that involves substrate coordination and intermediate formation of an arene complex, followed by CH cleavage. While ligand exchange reactions readily occur via the trans-five-coordinate intermediate, **R−Ir−□**, both experimental and theoretical results are consistent with the CH activation reaction requiring further reaction of **R−Ir−□** to generate the cis-intermediate, ***cis*-R−Ir−□**, before reaction. Experimental and theoretical studies are consistent with the formation of this species constituting the bulk of the barrier for the CH activation reactions and serve to explain why the rates of trans−cis isomerization and CH activation are comparable. Overall the CH activation reaction with **R−Ir−Py** has been shown to proceed via four key steps: (A)

a pre-equilibrium loss of pyridine that generates a trans-five-coordinate, square pyramidal intermediate, **R**−**Ir**−□, (B) a largely rate-determining, unimolecular, isomerization of the trans-five-coordinate to generate a five-coordinate intermediate, ***cis*-R**−**Ir**−□, (C) coordination of benzene to this species to generate a discrete benzene complex, ***cis*-R**−**Ir**−**PhH**, and (D) a rapid C−H cleavage step. Kinetic isotope effects on the CH activation comparing reaction with a mixture of C_6H_6/C_6D_6 (KIE = 1) and 1,3,5-$C_6H_3D_3$ (KIE ∼3) are consistent with the CH activation occurring via rate-determining arene coordination, followed by rapid CH cleavage.

In addition to showing that common O-donor ligands can be utilized in the design of efficient, stable CH activation catalysts capable of functionalization reactions, these studies show that the use of readily available, bis-chelating O-donor ligands, based on the acac-O,O ligands, may be used to access coordination reactions, such as CH activation, that require two mutually cis sites for reaction. These O-donor complexes are effective hydroarylation catalysts, and it will be interesting to rationalize the results of the current studies with the various catalytic steps of the hydroarylation reaction. For example, if mutually cis sites are required for the olefin insertion step, then the rate of the trans−cis isomerization could be expected to be a lower limit for the catalytic rate starting from the trans-complex while the rate for loss of pyridine would be expected to be the lower limit starting from the cis-complex. Other interesting aspects of these complexes, such as why no olefin products are observed in these catalytic reactions, will also be examined.

4. Experimental Section

4.1. General Considerations. Spectroscopy. Liquid phases of the organic products were analyzed with a Shimadzu GC-MS QP5000 (ver. 2) equipped with a cross-linked methyl silicone gum capillary column, DB5. Gas measurements were performed using a GasPro column. The retention times of the products were confirmed by comparison to standards. NMR spectra were obtained on a Bruker AC-250 (250.134 MHz for ^{1}H and 62.902 MHz for ^{13}C), a Bruker AM-360 (360.138 MHz for ^{1}H and 90.566 MHz for ^{13}C), or a Varian Mercury 400 (400.151 MHz for ^{1}H and 100.631 MHz for ^{13}C) spectrometer. Chemical shifts are given in ppm relative to TMS or to residual solvent proton resonances. All carbon resonances are singlets unless otherwise mentioned. Resonances due to pyridine are reported by chemical shift and multiplicity only. All pyridine complexes showed similar coupling constants (^3J = 5.00 Hz, ^4J = 1.5 Hz, *o-H* py; ^3J = 8.0 Hz, ^4J = 1.5 Hz, *p-H* py; ^3J = 6.50 Hz, *m-H* py). The temperature of the probe was monitored using methanol or ethylene glycol samples with an added trace of concentrated aqueous hydrochloric acid. Errors in reported temperatures are ±2 °C at a maximum. Fast atom bombardment (FAB^+) mass spectrometry was carried out using a VG ZAB-SE, high resolution double-focusing mass spectrometer at PASAROW Mass Spectrometry laboratory at UCLA using nitrobenzene alcohol (NBA) as the matrix.

X-ray diffraction data were collected on a Bruker SMART APEX CCD diffractometer with graphite monochromated Mo Kα radiation (λ = 0.710 73 Å). The cell parameters were obtained from the least-squares refinement of the spots (from 60 collected frames) using the program SMART. A hemisphere of data was collected up to a resolution of 0.75 Å. The intensity data were processed using the program Saint-Plus. All calculations for the structure determination were carried out using the SHELXTL package (version 5.1).[35] Initial atomic coordinates of the Ir atoms were located by direct methods, and structures were refined by least-squares methods. Empirical absorption corrections were applied using the program SADABS.[36] Calculated hydrogen positions were input and refined in a riding manner along with their attached carbons. A summary of the refinement details and the resulting parameters are given in the Supporting Information.

Materials and Analyses. All manipulations were carried out using glovebox and high vacuum line techniques. Benzene, benzene-d_6, toluene-d_8, and THF were purified by vacuum transfer from sodium benzophenone ketyl. CD_2Cl_2 and pyridine were dried by vacuum transfer from CaH_2. Synthetic work involving iridium complexes was carried out in an inert atmosphere despite the air stability of the complexes. Reagent-grade chemicals and solvents were used as purchased from Aldrich or Strem. Complex **[acac-C**−**Ir]$_2$**,[19] **acac-C**−**Ir**−**H$_2$O**,[16a] **acac-C**−**Ir**−**Py**,[16a] **Ph**−**Ir**−**H$_2$O**,[16a] **Ph**−**Ir**−**Py**,[16a] diethylmercury,[37] and bis(2-phenethyl)mercury[38] were prepared as described in the literature. Elemental analyses were done by Desert Analytics laboratory, Arizona.

[Ir(μ-acac-O,O,C^3)(acac-O,O)(CH$_3$)]$_2$ [CH$_3$−**Ir]$_2$: Method A:** In the glovebox, a Schlenk flask fitted with a Teflon valve was charged with **acac-C**−**Ir**−**H$_2$O** (342 mg, 0.675 mmol) and suspended in THF (100 mL). To this, was added a toluene solution of $ZnMe_2$ (2.0 M toluene, 370 μL, 0.740 mmol). Upon addition, the solution developed a slight orange color. The flask was then sealed, removed from the glovebox, and placed in a 60 °C oil bath for 2 h. The resulting slightly cloudy orange solution was cooled to room temperature, whereby a small amount of a white precipitate settled. The solution was poured onto water (200 mL), extracted with CH_2Cl_2 (2 × 100 mL), and then dried over Na_2SO_4. Filtration followed by removal of solvent in vacuo yielded a solid. Addition of acetone and precipitation with ether at −25 °C afforded a bright yellow solid. The clear yellow solution was decanted and the solid dried in vacuo, to afford **[CH$_3$**−**Ir]$_2$** as an analytically pure bright yellow powder (205 mg, 75% yield). Comparable yields were obtained when **[acac-C**−**Ir]$_2$** was used.

Method B: A solution of **acac-C**−**Ir**−**H$_2$O** (340 mg, 0.674 mmol) in methanol was added to a Schlenk flask fitted with a Teflon valve. To this, dimethylmercury (55 μL, 0.7 mmol) was added through a syringe. The reaction flask was heated to 60 °C for 2 h and then cooled to room temperature. The resulting solution was vacuum transferred to leave a crude orange powder. The crude reaction mixture was loaded on a silica gel column and eluted with THF to afford **[CH$_3$**−**Ir]$_2$** as yellow powder (220 mg, 80% yield).

^{1}H NMR ($CDCl_3$, rt): Due to the fluxional nature of the dinuclear complex in $CDCl_3$ at ambient temperature, the bridging and nonbridging acac resonances are broadened. δ 5.40 (br s, 4H, acac-C^3*H*), 1.96 (s, 6H, Ir−C*H*$_3$), 1.83 (br s, 24H, acac-C*H*$_3$). ^{1}H NMR ($CDCl_3$, −33 °C): δ 5.50 (s, 2H, O-acac-C^3*H*), 5.34 (s, 2H, μ-acac-C^3*H*), 1.89 (s, 6H, Ir−C*H*$_3$), 1.88 (s, 12H, O-acac-C*H*$_3$), 1.77 (s, 12H, μ-acac-C*H*$_3$). ^{13}C{^{1}H} ($CDCl_3$, −27 °C): δ 191.55 (μ-acac C═O), 183.14 (O-acac C═O), 103.79 (O-acac-*C*^{3}H), 81.56 (μ-acac-*C*^{3}H), 28.53 (μ-acac-*C*H$_3$), 27.32 (O-acac-*C*H$_3$), 21.31 (Ir−*C*H$_3$). ^{1}H NMR (CD_3OD): δ 5.46 (s, 2H, C^3*H*), 1.76 (s, 12H, acac-C*H*$_3$), 1.75 (s, 3H, C*H*$_3$). ^{13}C{^{1}H} NMR (CD_3OD): δ 184.3 (acac *C*═O), 103.8 (acac-*C*^{3}H), 26.4 (acac-*C*H$_3$), −34.9 (*C*H$_3$). Anal. Calcd for $C_{22}H_{34}Ir_2O_8$: C, 32.58; H, 4.23. Found: C, 31.87; H, 3.94.

[Ir(μ-acac-O,O,C^3)(acac-O,O)(CH$_2$CH$_2$Ph)]$_2$ [PhCH$_2$CH$_2$−**Ir]$_2$: [PhCH$_2$CH$_2$**−**Ir]$_2$** was synthesized according to Method B with **acac-C**−**Ir**−**H$_2$O** (100 mg, 0.197 mmol) in 10 mL of methanol and using bis(2-phenethyl)mercury (100 μL, 0.25 mmol). The crude reaction mixture was purified using column chromatography (silica gel) using a gradient solvent (100% THF to 1:1 THF−ether) and recrystallized from a mixture of CH_2Cl_2 and hexanes. The title compound was isolated as an orange powder (60 mg, 60% yield). ^{1}H NMR ($CDCl_3$): (−10

(35) Sheldrick, G. M. *SHELXTL*, version 5.1; Bruker Analytical X-ray System, Inc.: Madison, WI, 1997.

(36) Blessing, R. H. *Acta Crystallogr*. **1995**, *A51*, 33.

(37) Gilman, H.; Brown, R. E. *J. Am. Chem. Soc*. **1929**, 51, 928.

(38) (a) Criegee, R.; Dimorth, P.; Schempf, R. *Chem. Ber*. **1957**, *90*, 1337. (b) Rozema, M. J.; Rajagopal, D.; Tucker, C. E.; Knochel, P. *J. Organomet. Chem*. **1992**, *438*, 11. (c) Gilman, H.; Brown, R. E. *J. Am. Chem*. Soc. **1929**, *51*, 928.

°C) δ 7.1−7.35 (m, 10H, Ph), 5.52 (s, 2H, O-acac-C^3*H*), 5.42 (s, 2H, μ-acac-C^3*H*), 3.10 (m, 4H, Ph-CH_2), 2.3 (m, 4H, Ir−CH_2), 1.92 (s, 12H, O-acac-CH_3), 1.85 (s, 12H, μ-acac-CH_3). ^{13}C{^{1}H} ($CDCl_3$, −10 °C): δ 191.53 (μ-acac C═O), 183.19 (O-acac C═O), 143.35 (Ph), 128.37 (Ph), 128.32 (Ph), 125.32 (Ph), 104.05 (O-acac-*C*^{3}H), 82.19 (μ-acac-*C*^{3}H), 37.05 (Ph−*C*H_2), 28.69 (μ-acac-*C*H_3), 27.36 (O-acac-*C*H_3), 4.16 (Ir−*C*H_2). ^{1}H NMR (CD_3OD): δ 7.05−7.15 (m, 5H, Ph), 5.50 (s, 2H, acac-C^3*H*), 3.02 (m, 2H, Ph-CH_2), 2.05 (m, 2H, Ir−CH_2), 1.79 (s, 12H, acac-CH_3). ^{13}C{^{1}H}(CD_3OD): δ 184.2 (acac *C*═O), 146.1 (Ph), 128.9 (Ph), 125.5 (Ph), 103.9 (acac-*C*H), 38.9 (*C*H_2−Ph), 26.6 (acac-*C*H_3), −8.5 (Ir−*C*H_2). Anal. Calcd for $C_{34}H_{46}O_8Ir_2$: C, 42.22; H, 4.79. Found: C, 42.68; H, 4.48.

[Ir(μ-acac-O,O,C^3)(acac-O,O)(CH$_2$CH$_3$)]$_2$[CH$_3$CH$_2$−Ir]$_2$: [CH$_3$CH$_2$−Ir]$_2$ was synthesized similarly from **acac-C−Ir−H$_2$O** (200 mg, 0.394 mmol) and diethylzinc (360 μL, 1.1 M in toluene) using Method A or using diethylmercury (43 μL, 0.4 mmol) using Method B. **[CH$_3$CH$_2$−Ir]$_2$** was isolated in 75−80% yields. ^{1}H NMR ($CDCl_3$, −10 °C): δ 5.47 (s, 2H, O-acac-C^3*H*), 5.37 (s, 2H, μ-acac-C^3*H*), 2.87 (q, ^3J = 7.4 Hz, 4H, Ir−*C*H_2), 1.86 (s, 12H, O-acac-C*H*$_3$), 1.76 (s, 12H, μ-acac-C*H*$_3$), 0.31 (t, 6H, ^3J = 7.4 Hz, *C*H$_3$). ^{13}C{^{1}H} ($CDCl_3$, −10 °C): δ 190.67 (μ-acac C═O), 182.73 (O-acac C═O), 103.87 (O-acac-*C*^{3}H), 83.11 (μ-acac-*C*^{3}H), 28.56 (μ-acac-*C*H$_3$), 27.37 (O-acac-*C*H$_3$), 15.79 (*C*H$_3$), −4.44(Ir−*C*H_2).

[Ir(O,O-acac)$_2$(CH$_3$)(Py)] (CH$_3$−Ir−Py): CH$_3$−Ir−Py was synthesized similarly from **[CH$_3$−Ir]$_2$** (100 mg, 0.123 mmol) in $CHCl_3$ and pyridine (1 mL, 12.3 mmol). Isolated yield: 115 mg, >95%. ^{1}H NMR and ^{13}C{^{1}H} NMR were consistent with earlier reports.[15] FAB$^+$ MS: *m*/*z* (%) 485.1 (8) [M$^+$], 406.1 (100) [M−Py]$^+$, 391.1 (14) [M−Py−CH$_3$]$^+$.

[Ir(O,O-acac)$_2$(CH$_2$CH$_2$Ph)(Py)] (PhCH$_2$CH$_2$−Ir−Py). PhCH$_2$CH$_2$−Ir−Py was synthesized similarly from **[PhCH$_2$CH$_2$−Ir]$_2$** (100 mg, 0.206 mmol) in 10 mL of methanol and pyridine (1 mL, 12.3 mmol). Isolated yield: 120 mg, >95%. ^{1}H NMR (CD_2Cl_2): δ 8.41 (d, 2H, *o*-*H* Py), 7.83 (t, 1H, *p*-*H* Py), 7.39 (t, 2H, *m*-*H* Py), 7.20 (m, 4H, Ph), 7.07 (m, 1H, Ph), 5.27 (s, 2H, acac-C^3*H*), 2.75 (m, 2H, Ph-CH_2), 2.24 (m, 2H, Ir−CH_2), 1.75 (s, 12H, acac-CH_3). ^{13}C {^{1}H} NMR (CD_2Cl_2): δ 183.6 (acac *C*═O), 149.6 (*o*-Py), 137.2 (*p*-Py), 128.3 (Ph), 128.1 (Ph), 125.0 (*m*-Py), 124.5 (Ph), 103.2 (acac *C*^{3}H), 37.4 (*C*H_2—Ph), 27.2 (acac *C*H_3), −2.4 (*C*H_2—Ir). Anal. Calcd for $C_{23}H_{28}NO_4Ir$: C, 48.07; H, 4.91; N, 2.44. Found: C, 48.24; H, 4.75; N, 2.54. FAB$^+$ MS: *m*/*z* (%) 575.1 (13) [M$^+$], 496.1 (100) [M−Py]$^+$, 391.1 (16) [M−Py−CH$_2$−CH$_2$−Ph]$^+$.

[Ir(O,O-acac)$_2$(CH$_2$−CH$_3$)(Py)] (CH$_3$CH$_2$−Ir−Py): CH$_3$CH$_2$−Ir−Py was synthesized similarly from **[CH$_3$CH$_2$−Ir]$_2$** (100 mg, 0.119 mmol) in $CHCl_3$ and pyridine (1 mL, 12.3 mmol). Isolated yield: 110 mg, >95%. ^{1}H NMR (C_6D_6): δ 8.69 (d, 2H, *o*-*H* py), 6.80 (tt, 1H, *p*-*H* py), 6.60−6.75 (m, 2H, *m*-*H* py), 5.08 (s, 2H, acac-C^3*H*), 3.50 (q, ^3J = 7.6 Hz, −CH_2—Ir), 1.60 (s, 12H, acac-CH_3), 1.25 (t, 3H, ^3J = 7.6 Hz, C*H*$_3$—CH$_2$—Ir).^{13}C{^{1}H} NMR (C_6D_6): δ 182.69 (acac C═O), 149.57 (*o*-Py), 136.32 (*p*-Py), 124.38 (*m*-Py), 102.76 (acac-*C*^{3}H), 26.66 (acac-*C*H$_3$), 15.99 (*C*H$_3$), −10.56 (*C*H_2—Ir). Anal. Calcd for $C_{17}H_{24}NO_4Ir$: C, 40.95; H, 4.85; N, 2.81. Found: C, 41.38; H, 4.95; N, 2.70. FAB$^+$ MS: *m*/*z* (%) 499.1 (10) [M$^+$], 420.1 (100) [M−Py]$^+$, 391.1 (17) [M−Py−CH$_2$−CH$_3$]$^+$.

***cis*-[Ir(O,O-acac)$_2$(Ph)(Py)] (*cis*-Ph−Ir−Py):** A 3 mL stainless steel autoclave equipped with a glass insert and a magnetic stir bar was charged with 1 mL of benzene containing **Ph−Ir−Py** (10 mg, 0.02 mmol). The autoclave was pressurized with an additional 2.96 MPa of argon. The autoclave was heated for 12 h in a well-stirred heating bath maintained at 180 °C. The autoclave was cooled thereafter, and the solvent was transferred in a Schlenk flask, whereby the solvent was removed in vacuo. Isolated yield: 9 mg, >95%. ^{1}H NMR (CD_2Cl_2): δ 8.21 (d, 2H, *o*-*H* py), 7.71 (t, 1H, *p*-*H* py), 7.17 (t, 2H, *m*-*H* py), 6.88 (t, 2H, *m*-*H* Ph), 6.82 (t, 1H, *p*-*H* Ph), 6.71 (d, 2H, *o*-*H* Ph), 5.34 (s, 1H, acac-C^3*H*), 5.29 (s, 1H, acac-C^3*H*), 1.94 (s, 3H, acac-C*H*$_3$), 1.87 (s, 6H, acac-C*H*$_3$), 1.77 (s, 3H, acac-C*H*$_3$). ^{13}C{^{1}H} NMR (CD_2Cl_2): δ 186.48 (acac *C*═O), 185.80 (acac *C*═O), 184.67 (acac *C*═O), 184.21 (acac *C*═O). Phenyl and pyridine carbons: 171.07, 154.41, 137.21, 136.98, 131.20, 129.30, 128.84, 126.03, 125.05, 122.76, 102.72 (acac-*C*^{3}H), 101.30 (acac-*C*^{3}H), 28.75 (acac-*C*H$_3$), 27.91 (acac-*C*H$_3$), 27.37 (acac-*C*H$_3$), 27.26 (acac-*C*H$_3$). Anal. Calcd for $C_{21}H_{24}NO_4Ir$: C, 46.14; H, 4.43; N, 2.56. Found: C, 46.08; H, 4.55; N, 2.50.

Line Broadening Studies. The mononuclear−dinuclear equilibrium was measured in the slow exchange region from the width of the NMR signals at half-height using the equation $1/\tau_a = \pi(\omega_A - \omega^\circ_A)$, where τ_a is the residence time in site A and ω_A and ω°_A are the line widths in the presence and in the absence of exchange, respectively. ω°_A was measured at a temperature where the signals were not exchanging on the NMR time scale. The experimental line widths were corrected by subtracting the line width of TMS to minimize the effect of instrumental line-broadening. Values of the rate constants at various temperatures were used to obtain $\Delta G^\ddagger$ and the Arrhenius parameters using the Eyring plot.

Pyridine Exchange Studies with Ph−Ir−Py and CH$_3$−Ir−Py. A stock solution of **Ph−Ir−Py** or **CH$_3$−Ir−Py** in $CDCl_3$ (5 mM) was made and transferred to four oven-dried NMR tubes. Py-d_5 (52−156 mM) was added to these NMR tubes at low temperature and then subjected to precooled (273 K) NMR studies. The intensity of the bound or free pyridine was plotted against time using the Mercury 400 NMR machine.

Kinetics for CH Activation of C$_6$D$_6$ with CH$_3$−Ir−Py at Constant [C$_6$D$_6$/Py]: A stock solution of **CH$_3$−Ir−Py** was made in C_6D_6 (17 mM) with added pyridine-d_5 (510 mM) and trimethoxybenzene (5 mg) as internal standard. A 200 μL aliquot of this solution was added to a 5 mm thick J-young NMR tube fitted with a valve to which argon (100−150 psig) was added. The NMR tube was heated in a well-stirred oil bath maintained at a temperature (140−180 °C) during which the sample was analyzed by ^{1}H NMR spectroscopy. The reaction was monitored for 3 half-lives.

Dependence of Trans−Cis Isomerization of Ph−Ir−Py on Pyridine Concentration: A stock solution of **Ph−Ir−Py** in C_6D_6 (15 mM) with trimethoxybenzene (1 mM) as internal standard was added to three 5 mm J-young NMR tubes fitted with a valve. To each of them, Py-d_5, ranging from 0.5 to 2.5 molar equiv, was added. The NMR tube was heated with added argon pressure (100−150 psig) in a well-stirred oil bath maintained at 180 °C during which the samples were analyzed by ^{1}H NMR spectroscopy. The reactions were monitored for 2−3 half-lives.

Dependence of Benzene CH Activation on Pyridine Concentration: A stock solution of **PhCH$_2$CH$_2$−Ir−Py** in C_6D_6 (15 mM) with trimethoxybenzene (1 mM) as internal standard was added to three 5 mm J-young NMR tubes fitted with a valve. To each of them, Py-d_5, ranging from 72 mM to 217 mM was added. The NMR tube were heated with added argon pressure (100−150 psig) in a well-stirred oil bath maintained at 140 °C during which the samples were analyzed by ^{1}H NMR spectroscopy. The reaction was monitored for 2−3 half-lives.

Arene Concentration Dependence on Rate of C−H Activation of Benzene with Cy-d_{11}−Ir−Py: Cy-d_{11}−Ir−Py (5 mg) along with trimethoxybenzene (1 mg) as internal standard was added to three 5 mm J-young NMR tubes fitted with a Teflon valve. To these, varying amounts of C_6D_6 and C_6D_{12} were added {[C_6D_6] = 1600−5600 mM}. The NMR tubes were heated with added argon pressure (100−150 psig) in a well-stirred oil bath maintained at 120 °C during which the samples were analyzed by ^{1}H NMR spectroscopy. The reactions were monitored for 2−3 half-lives. After the reaction, CD_2Cl_2 was added to dissolve all **Ph-d_5−Ir−Py** produced, and the trimethoxybenzene was used as an internal standard to ensure that **Ph-d_5−Ir−Py** produced accounted for >95% of the added **Cy-d_{11}−Ir−Py**.

Deuterium Kinetic Isotope Effect on Arene C−H Activation with CH$_3$−Ir−Py: Three 2 mL thick glass screw cap vials containing septa were loaded with 5 mg (0.01 mmol) of **CH$_3$−Ir−Py** in parallel. To these vials, 0.5 mL of C_6D_6, 1,3,5-$C_6H_3D_3$ and a 1:1 molar mixture of

C_6H_6 and C_6D_6 were introduced. The vials were freeze−pump−thawed thrice and filled with argon gas. The vials were immersed in a 110 °C oil bath, and the gas phase was sampled for 3 half-lives and analyzed on a GC−MS equipped with a Gas Pro column. The molar ratio of the liberated methane isotopomers was deconvoluted using a spreadsheet. The solution remained homogeneous throughout the reaction, and no signs of decomposition were observed. The liquid phase was analyzed to make sure that no deuterium scrambling had occurred.

H−D Exchange between C_6H_6 and Toluene-d_8: Catalytic H−D exchange reactions were quantified by monitoring by the increase of deuterium into C_6H_6 by GC/MS analyses for **Ph−Ir−Py** and ***cis*-Ph−Ir−Py** (5 mM) using toluene-d_8 as the deuterium source at 160 °C. This was achieved by deconvoluting the mass fragmentation pattern obtained from the MS analysis, using a program developed on Microsoft EXCEL. The mass range from 78 to 84 (for benzene) was examined for each reaction and compared to a control reaction where no metal catalyst was added. The program was calibrated with known mixtures of benzene isotopomers. The results obtained by this method are reliable to within 5%. Catalytic H/D exchange reactions were thus run for reaction times in order to be able to detect changes >5% in exchange.

Computational Methodology: All calculations were performed using the hybrid DFT functional B3LYP as implemented by the Jaguar 5.0 or 5.5 program package.[39] This DFT functional utilizes the Becke three-parameter functional[40] (B3) combined with the correlation functional of Lee, Yang, and Par[41] (LYP) and is known to produce good descriptions of reaction profiles for transition-metal-containing compounds.[42,43] The iridium was described by the Wadt and Hay[44] core-valence (relativistic) effective core potential (treating the valence electrons explicitly) using the LACVP basis set with the valence double-ζ contraction of the basis functions, LACVP**. All electrons were used for all other elements using a modified variant of Pople's[45] 6-31G** basis set, where the six d functions have been reduced to five.

Implicit solvent effects of the experimental benzene medium were calculated with the Poisson−Boltzmann (PBF) continuum approximation,[46] using the parameters $\epsilon = 2.284$ and $r_{solv} = 2.602$ Å. Due to the increased cost of optimizing systems in the solvated phase (increase in computation time by a factor of ∼4) solvation effects were calculated here as single-point solvation corrections to gas-phase geometries, except for cases where a vacant coordination site is created. Allowing relaxation in solvent did not change the relative energies more than 1 kcal/mol for species where the coordination remained constant; however, in cases where the coordination changed, the relaxation can account for up to 4 kcal/mol.

All geometries were optimized and evaluated for the correct number of imaginary frequencies through vibrational frequency calculations using the analytic Hessian. Zero imaginary frequencies correspond to a local minimum, while one imaginary frequency corresponds to a transition structure.

To reduce computational time, the methyl groups on the acac ligands were replaced with hydrogens. Control calculations show that relative energies of intermediates and transition structures change less than 0.1 kcal/mol when methyl groups are included.

Acknowledgment. We gratefully acknowledge financial support of this research by the Chevron Texaco Energy Research and Technology Co. and thank Dr. William Schinski of Chevron Texaco for helpful discussions. The authors would also like to thank Ms. Irina Tysba, Mr. NamHat Ho, Mr. Muhammed Yousufuddin, and Prof. Bau for X-ray crystallography. We thank David Laviska of Rutgers, The State University of New Jersey for helping with the editing of this manuscript.

Supporting Information Available: First-order plots and activation parameters for line-broadening analysis, Py exchange, and CH activation, and crystal data for **Ph−Ir−Py** and **Ph−CH_2−CH_2−Ir−Py**. This material is available free of charge via the Internet at http://pubs.acs.org.

JA051532O

(39) *Jaguar 5.0*; Schrodinger, Inc.: Portland, Oregon, 2000.
(40) Becke, A. D. *J. Chem. Phys.* **1993**, *98*, 5648.
(41) Lee, C.; Yang, W.; Parr, R. G. *Phys. Rev. B* **1988**, *37*, 785.
(42) Baker, J.; Muir, M.; Andzelm, J.; Scheiner, A. *In Chemical Applications of Density-Functional Theory*; Laird, B. B., Ross, R. B., Ziegler, T., Eds.; ACS Symposium Series 629; American Chemical Society: Washington, DC, 1996.
(43) Niu, S.; Hall, B. M. *Chem. Rev.* **2000**, *100*, 353.
(44) (a) Hay, P. J.; Wadt, W. R. *J. Chem. Phys.* **1985**, *82*, 299. (b) Goddard, W. A., III. *Phys. Rev.* **1968**, *174*, 659. (c) Melius, C. F.; Olafson, B. O.; Goddard, W. A., III. *Chem. Phys. Lett.* **1974**, *28*, 457.
(45) (a) Hariharan, P. C.; Pople, J. A. *Chem. Phys. Lett.* **1972**, *16*, 217. (b) Francl, M. M.; Pietro, W. J.; Hehre, W. J.; Binkley, J. S.; Gordon, M. S.; DeFrees, D. J.; Pople, J. A. *J. Chem. Phys.* **1982**, *77*, 3654.
(46) (a) Tannor, D. J.; Marten, B.; Murphy, R.; Friesner, R. A.; Sitkoff, D.; Nicholls, A.; Ringnalda, M.; Goddard, W. A., III; Honig, B. *J. Am. Chem. Soc.* **1994**, *116*, 11875. (b) Marten, B.; Kim, K.; Cortis, C.; Friesner, R. A.; Murphy, R. B.; Ringnalda, M. N.; Sitkoff, D.; Honig, B. *J. Phys. Chem.* **1996**, *100*, 11775.